1000-0569/2016/032(03)-0629-45 *Acta Petrologica Sinica* 岩石学报

Zircon U-Pb age, geochemical, and Sr-Nd-Hf isotopic constraints on the origin of Early Cretaceous mafic dykes from western Shandong Province, eastern North China Craton, China

华北克拉通东部鲁西早白垩纪基性岩墙成因:来自锆石年龄、地球化学和 Sr-Nd-Hf 同位素的证据*

LIU Shen[1,2], FENG CaiXia[1], ZHAI MingGuo[1], HU RuiZhong[2], LAI ShaoCong[1], CHEN JunJin[3] and YAN Jun[2]

刘燊[1,2] 冯彩霞[1] 翟明国[1] 胡瑞忠[2] 赖绍聪[1] 陈俊瑾[3] 颜军[2]

1. *State Key Laboratory of Continental Dynamics, Department of Geology, Northwest University, Xi'an* 710069, *China*
2. *State Key Laboratory of Ore Deposit Geochemistry, Institute of Geochemistry, Chinese Academy of Sciences, Guiyang* 550002, *China*
3. *No. 6 Gold Geological Party of CAPF, Xining* 810021, *China*
1. 大陆动力学国家重点实验室,西北大学地质学系,西安 710069
2. 矿床地球化学国家重点实验室,中国科学院地球化学研究所,贵阳 550002
3. 青海省西宁市武警黄金第六支队,西宁 810021

Received: 2014-10-30, Accepted: 2015-02-02.

Liu S, Feng CX, Zhai MG, Hu RZ, Lai SC, Chen JJ and Yan J. 2016. Zircon U-Pb age, geochemical, and Sr-Nd-Hf isotopic constraints on the origin of Early Cretaceous mafic dykes from western Shandong Province, eastern North China Craton, China. *Acta Petrologica Sinica*, 32(3): 629-645

Abstract Mesozoic mafic doleritic dykes form swarms that are widespread across Shandong Province in the eastern North China Craton (NCC). We present U-Pb zircon ages, geochemical data, and Sr-Nd-Hf isotopic data for representative samples of these dykes. U-Pb zircon analyses for four samples, using laser ablation-inductively coupled plasma-mass spectrometry (LA-ICP-MS), yielded ages that range from 121.9 ± 0.6 to 124.3 ± 0.5Ma (Early Cretaceous time). The dolerites are characterised by a narrow range of rock compositions. They display enrichments in light rare earth elements and large ion lithophile elements (i.e., Rb, Ba, U, K and Pb), as well as depletion in high field strength elements (Nb, Ta and Ti). The mafic dykes have uniform $(^{87}Sr/^{86}Sr)_i$ values of ~0.7098, low $\varepsilon_{Nd}(t)$ values in the range of −14.7 to −14.5, $\varepsilon_{Hf}(t)$ values (for zircon) are between −31.4 and −26.7 and high hafnium model ages (t_{DM1} = 1817 ~ 2024Ma). These results indicate that the mafic dykes were derived from partial melting of an enriched, lithospheric mantle source. The magmas underwent direct crustal contamination. In summary, the origin of the dykes can be attributed to the collision between the NCC and the Yangtze Craton, the magmas that formed these dykes were sourced from a hybridized source caused by subduction of Yangtze crustal sedimentary material beneath southeastern before the Late Mesozoic.

Key words Mafic dykes; Foundering; Western Shandong Province; NCC

摘 要 中生代基性辉绿岩墙广泛分布于华北克拉通东部山东地区。本研究给出代表性岩墙的 U-Pb 锆石年龄、地球化学和 Sr-Nd-Hf 同位素证据,4 个代表性锆石的 LA-ICP-MS 年龄范围处于 121.9 ± 0.6Ma 和 124.3 ± 0.5Ma 之间(早白垩纪)。岩石的主量元素组成变化较小,岩石富集轻稀土元素和大离子亲石元素(如,Rb、Ba、U、K 和 Pb),以及亏损高场强元素(如,Nb、Ta 和 Ti)。另外,基性岩墙具有相对一致的$(^{87}Sr/^{86}Sr)_i$比值(~0.7098),负的 $\varepsilon_{Nd}(t)$ 值(−14.7 ~ −14.5)、$\varepsilon_{Hf}(t)$ 值(−31.4 ~ −26.7)和高的 Hf 模式年龄(t_{DM1} = 1817 ~ 2024Ma)。研究显示基性岩墙来自富集岩石圈地幔的部分熔融作用,并在上升侵位过程中经历了一定程度的地壳混染作用影响。总体研究表明,基性岩墙的成因机制与扬子克拉通与华北克拉通的碰撞有关,岩浆源区为晚中生代前受俯冲扬子地壳沉积物交代后的富集岩石圈地幔。

关键词 基性岩墙; 拆沉; 鲁西; 华北克拉通

中图法分类号 P588.124; P597.3

* This research was supported by the Opening Project of the State Key Laboratory of Ore deposit Geochemistry (201206), and National Natural Science Foundation of China (41373028, 41573022).

The First Author: Prof. Liu Shen, 1974, igneous rocks and geochemistry, E-mail: liushen@nwu.edu.cn

1 Introduction

Mafic dykes, ranging in size from tens to several hundreds of metres thickness and from several to many hundreds or even thousands of kilometres in length, have been emplaced in many parts of the world in response to regional-scale lithospheric extension that commonly accompanies the initial stages of the breakup of supercontinents (Halls, 1982; Halls and Fahrig, 1987; Féraud *et al.*, 1987; Tarney and Weaver, 1987; Zhao and McCulloch, 1993; Gudmundsson, 1995; Hou *et al.*, 2006; Liu, 2004; Liu *et al.*, 2004, 2005, 2006, 2008a, b, c, 2009a, b, 2012a, b, 2013a, b, c, d, e; Peng, 2010; Peng *et al.*, 2005, 2007, 2008, 2010, 2011a, b). The compositions of these mafic dykes include basalt, dolerite, gabbro, dolerite-porphyry, picrite, norite and lamprophyre. Examples of continental-scale suites of mafic dykes include the Kennedy and San Rafael mafic dykes; the Mackenzie, Matachewan, Mistassini, Franklin, Grenville and Marathon dyke swarms of Canada (Halls and Hatts, 1990; Ernst *et al.*, 1992, 1995, 2005; Liu *et al.*, 2013c); the Great Dyke of Zimbabwe (Oberthür *et al.*, 2002); the Jimberland and Widgiemooltha mafic dykes of Australia (Ma *et al.*, 2000); and the southwestern Greenland mafic dykes (Nisson *et al.*, 2013). Other important occurrences of mafic dykes include swarms from Brazil, India, Italy, Japan, Norway, Scotland, Siberia, South Africa and China (e.g., the southern China and NCC; Hou *et al.*, 2006; Liu, 2004; Liu *et al.*, 2004, 2005, 2006, 2008a, b, 2009a, b, 2012a, b, 2013a, b, c, d, e; Peng, 2010; Peng *et al.*, 2005, 2007, 2008, 2010, 2011a, b; Chen *et al.*, 2015). And the swarms of mafic dykes have very old ages (> 2.5 ~ 1.0Ga).

In terms of China, workers to date have focused primarily on the mafic dykes of Proterozoic age in both of the southern China and NCC (e.g., Chen and Shi, 1983, 1994; Chen *et al.*, 1992; Peng *et al.*, 2005, 2007, 2008, 2010, 2011a, b; Hou *et al.*, 2006; Piper *et al.*, 2011; Li *et al.*, 2010; Liu *et al.*, 2012b, 2013b, c; Peng, 2010). However, in addition to these older mafic dykes, many mafic dykes of Mesozoic age occur across China. For example, in southern China (e.g., Zhejiang, Jiangxi, Hunan, Fujian, Guangdong, Guangxi and Hainan provinces), more than 700 dykes have been recorded, while a similar number crop out over the entire NCC (e.g., the Shandong, Liaoning, Jilin, Shanxi, Hebei and Inner Mongolia regions). While many studies have been carried out on these Mesozoic dykes, there are controversy regarding their petrogenesis and ages of emplacement (e.g., underplating, magma immiscibility, metathesis, delamination; 150 ~ 80Ma; Shao and Zhang, 2002; Zhang and Sun, 2002; Shao *et al.*, 2003; Xie, 2003; Zhai *et al.*, 2003, 2004; Liu, 2004; Xu, 2004; Yang *et al.*, 2004; Zhao, 2004; Liu *et al.*, 2005, 2006, 2008a, b, c, 2009a, b, 2012c, d, 2013a, d, e; Zhang, 2006; Cao, 2007; Wang *et al.*, 2007; Wu *et al.*, 2008; Zhang, 2009; Zhai and Santosh, 2013).

To further refine the ages and petrological models for Mesozoic mafic magmatism in China, a more detailed geochronological, geochemical and isotopic study of a variety of Mesozoic mafic dykes from southern China and the NCC is required. We therefore present here the results of new zircon U-Pb dating using LA-ICP-MS, as well as petrological, whole-rock geochemical, and Sr-Nd-Hf isotopic data for representative samples of mafic dykes from the Eastern Block of the NCC and the Zichuan region in western Shandong Province. These new data allow us to constrain the emplacement ages of these dykes and the origin of this mafic magmatism.

2 Geological setting and petrography

The NCC is located in northern China, covers a wide area ($\sim 170 \times 10^4 km^2$) (Wu *et al.*, 2008; Zhai and Santosh, 2011, 2013; Zheng *et al.*, 2013; Li *et al.*, 2013), and consists of Archaean Eastern and Western blocks which collided at ~1.85Ga along the nearly N-S-trending Palaeoproterozoic Trans-North China Orogen (Zhao *et al.*, 2001, 2005; Wilde *et al.*, 2002; Guo *et al.*, 2005). The Eastern and Western blocks can be further subdivided into microcontinental blocks and active belts (Zhai and Bian, 2000; Zhao, 2009). For example, the Western Block consists of the Yinshan Block in the north and the Ordos Block to the south, separated by the E-W-trending Palaeoproterozoic Khondalite Belt (Xia *et al.*, 2008; Yin *et al.*, 2009, 2011; Li *et al.*, 2011; Wang *et al.*, 2011). The Eastern Block consists of the Longgang (also known as the Yanliao Block) and Langrim blocks, separated by the Palaeoproterozoic Jiao-Liao-Ji Belt (Li *et al.*, 2006; Li and Zhao, 2007; Luo *et al.* 2008; Zhou *et al.*, 2008; Huang *et al.*, 2009; Wang *et al.*, 2009; Zhao *et al.*, 2010, 2012; Tam *et al.*, 2011, 2012a, b; Wu *et al.*, 2013a, b; Zhao and Zhai, 2013). The NCC is one of the oldest continents (Lin *et al.*, 2008) with a crustal age of >3.8Ga (Liu *et al.*, 1992), and its southern and northern margins are the Indosinian Qingling-Dabie and Hercynian Yinshan-Yanshan orogenic belts, respectively. Traditionally, the NCC has been considered to comprise uniform Precambrian (Archaean-Sinian) crystalline basement, overlain by a variety of younger cover lithologies of Cambrian-Quaternary age.

Shandong Province is located in the Eastern Block of the NCC, and more than 200 Mesozoic mafic dykes occur throughout eastern Shandong (Jiaodong), western Shandong (Luxi) and adjacent areas of Tan-Lu Fault. The study areas for this investigation are in the Zichuan region of western Shandong Province (samples SJ1 to SJ8, KJ1 to KJ4 and CN1 to CN4). The sampled mafic dykes from this area intrude Jurassic sedimentary rocks (JzS) and Proterozoic complexes (P) (Fig. 1). Individual dykes are vertical, trend NW-SE, are 15m to 0.8km wide, and 3.0 to 20km long (Fig. 1b). The dykes are typical medium-grained diabases that contain phenocrysts of clinopyroxene (2.0 ~ 6.5mm) and plagioclase (2.0 ~ 5.0mm) within a matrix (60% ~ 65%) of clinopyroxene (0.05 ~ 0.07mm) and plagioclase (0.03 ~ 0.06mm) with minor magnetite (ca. 0.02 ~ 0.04mm) and chlorite (0.04 ~ 0.05mm). Accessory minerals include zircon and apatite.

3 Analytical techniques

3.1 Zircon LA-ICP-MS U-Pb dating

Zircon was separated from four samples (SJ01, SJ02, KJ01 and CN01) using conventional heavy liquid and magnetic techniques at the Langfang Regional Geological Survey, Hebei

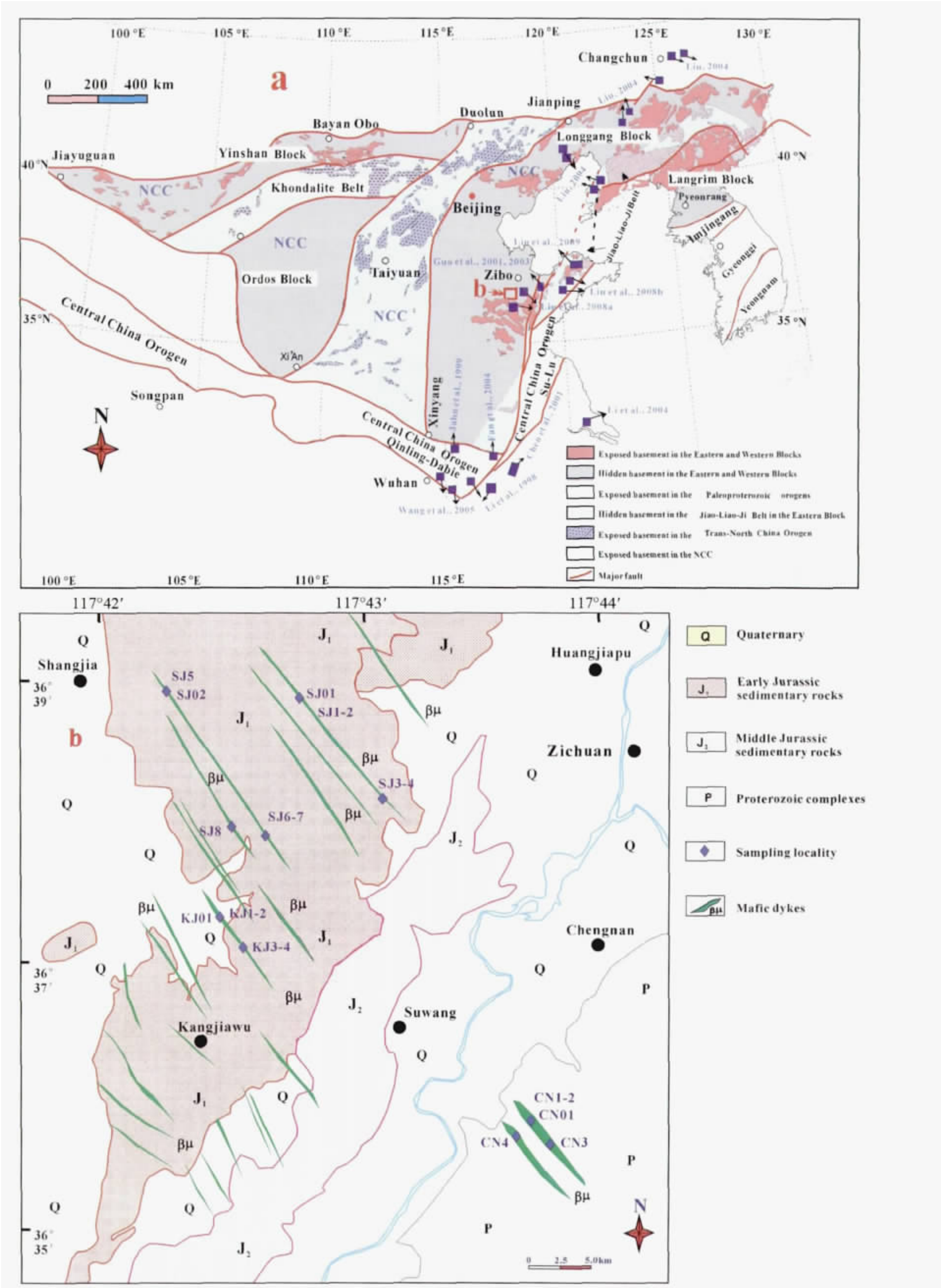

Fig. 1 Sketch map of study area and adjacent areas, China (a) and geological map of the study areas, showing the distribution of the mafic dykes and sampling localities (b)

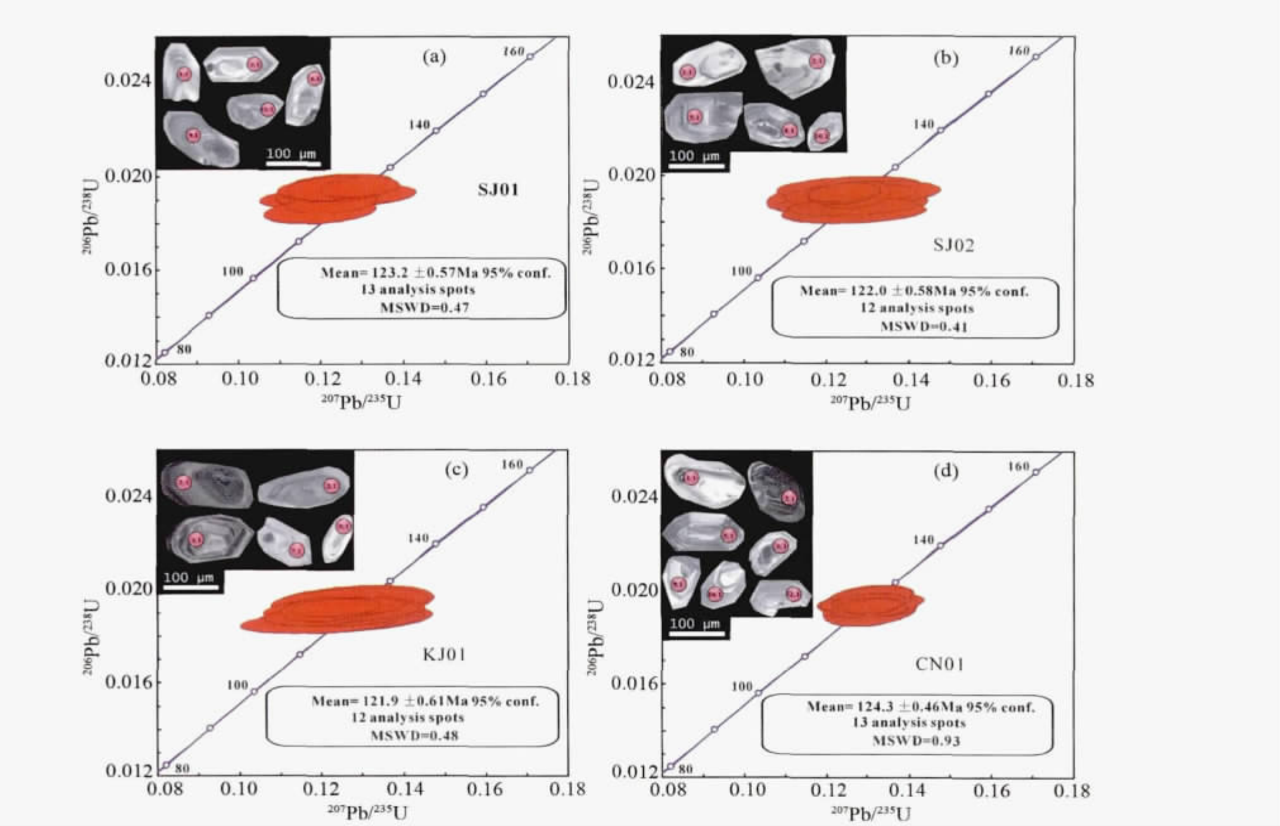

Fig. 2 Zircon LA-ICP-MS U-Pb concordia diagrams and CL images of zircons separated from the mafic dykes from western Shandong Province, China

Province, China. After separation and mounting, the internal and external structures of zircon grains were imaged using transmitted and reflected light, and cathodoluminescence at the State Key Laboratory of Continental Dynamics, Northwest University, China. Prior to zircon U-Pb dating, grain mount surfaces were rinsed in dilute HNO_3 and pure alcohol to remove any potential lead contamination. Zircon U-Pb ages were determined using LA-ICP-MS (Table1; Fig. 2) with an Agilent 7500a ICP-MS instrument equipped with a 193nm excimer laser at the State Key Laboratory of Geological Processes and Mineral Resources, China University of Geoscience (Wuhan), China. Zircon standard (#91500) was used for quality control, and the NIST 610 standard was used for data optimisation. A spot diameter of 24μm was used during analyses, employing the methodology described by Yuan *et al.* (2004) and Liu *et al.* (2010). Common Pb correction was undertaken following Andersen (2002), and the resulting data were processed using the GLITTER and ISOPLOT programs (Ludwig, 2003; Table1; Fig. 2). Uncertainties for individual LA-ICP-MS analyses are quoted at the 95% (2σ) confidence level.

3.2 Whole-rock geochemistry

The whole-rock and Sr-Nd isotope compositions of 16 samples were determined during this study. Prior to whole-rock geochemical analysis, samples were trimmed to remove altered surfaces, cleaned with de-ionised water, and then crushed and powdered in an agate mill. Major element concentrations were determined on fused glass discs using a PANalytical Axios-advance X-ray fluorescence spectrometer at the State Key Laboratory of Ore Deposit Geochemistry, Institute of Geochemistry, Chinese Academy of Sciences, China. These analyses have a precision of <5%, as determined using the GSR-1 and GSR-3 Chinese national standards (Table 2). Loss on ignition values was obtained using 1g of powder heated to 1100℃ for one hour (Table 2). Trace element concentrations were determined using ICP-MS at the State Key Laboratory of Ore Deposit Geochemistry, Institute of Geochemistry, Chinese Academy of Sciences, China, following the procedures outlined in Qi *et al.* (2000). Triplicate analyses were reproducible to within 5% for all elements, and analyses of the OU-6 (Potts and Kane, 2005) and GBPG-1 (Thompson *et al.*, 2000) international standards are agreed with recommended values (Table 3).

3.3 Sr-Nd isotope analyses

Sample powders used for Rb-Sr and Sm-Nd isotope analyses were spiked with mixed isotope tracers, dissolved in Teflon capsules with HF and HNO_3 acids, and separated by conventional cation-exchange techniques. Isotopic measurements were performed using a Finnigan Triton Ti thermal ionisation mass spectrometer at the State Key Laboratory of Geological Processes and Mineral Resources, China University of Geosciences (Wuhan), China. Procedural blanks yielded concentrations of <200pg for Sm and Nd, and <500pg for Rb

Table 1 LA-ICP-MS U-Pb isotope data for zircon separates from the mafic dykes of western Shandong Province

Spot No.	Th	U	Pb	Th/U	Isotopic ratio						Age (Ma)					
	($\times 10^{-6}$)				$^{207}Pb/^{206}Pb$	1σ	$^{207}Pb/^{235}U$	1σ	$^{206}Pb/^{238}U$	1σ	$^{207}Pb/^{206}Pb$	1σ	$^{207}Pb/^{235}U$	1σ	$^{206}Pb/^{238}U$	1σ
SJ01																
1	348	253	8.14	1.38	0.0472	0.0053	0.1225	0.0073	0.0189	0.0003	55	227	118	11	122	2
2	266	193	5.96	1.38	0.0585	0.0044	0.1197	0.0098	0.0191	0.0003	545	112	144	8	122	3
3	185	136	4.36	1.36	0.0582	0.0031	0.1236	0.0076	0.0193	0.0004	572	79	144	8	122	2
4	321	173	5.98	1.86	0.0581	0.0032	0.1205	0.0075	0.0195	0.0003	547	81	143	6	123	2
5	312	213	6.37	1.46	0.0504	0.0034	0.1304	0.0083	0.0192	0.0003	205	113	127	8	121	3
6	258	196	6.47	1.32	0.0462	0.0045	0.1223	0.0083	0.0194	0.0003	535	212	118	13	123	2
7	372	214	7.15	1.74	0.0464	0.0043	0.1197	0.0091	0.0185	0.0004	12	193	116	10	121	3
8	453	242	8.36	1.87	0.0553	0.0029	0.1236	0.0072	0.0193	0.0003	414	88	137	8	124	2
9	358	253	8.03	1.42	0.0472	0.0035	0.1218	0.0086	0.0192	0.0004	433	164	118	10	121	2
11	272	213	6.43	1.28	0.0485	0.0025	0.1292	0.0063	0.0195	0.0003	116	83	125	8	125	2
12	165	114	3.75	1.45	0.0573	0.0068	0.1248	0.0082	0.0197	0.0003	493	264	147	10	125	2
13	248	191	5.82	1.30	0.0575	0.0026	0.1221	0.0071	0.0195	0.0003	508	69	146	8	125	3
SJ02																
1	482	393	11.6	1.23	0.0486	0.0041	0.1263	0.0104	0.0187	0.0003	118	186	122	9	122	2
2	313	205	6.78	1.53	0.0535	0.0064	0.1283	0.0116	0.0193	0.0004	343	274	132	11	123	3
3	424	256	8.33	1.66	0.0561	0.0027	0.1246	0.0068	0.0193	0.0003	448	82	135	9	122	2
4	206	146	4.36	1.41	0.0554	0.0072	0.1266	0.0117	0.0185	0.0003	417	295	134	10	121	3
5	356	321	9.15	1.11	0.0535	0.0024	0.1268	0.0058	0.0192	0.0004	306	73	132	6	122	2
6	343	205	6.43	1.67	0.0587	0.0046	0.1246	0.0127	0.0191	0.0005	545	123	148	10	121	3
7	229	177	5.42	1.29	0.0583	0.0046	0.1303	0.0114	0.0193	0.0004	537	131	144	10	122	2
8	455	392	12.6	1.16	0.0516	0.0042	0.1256	0.0105	0.0192	0.0003	262	176	128	9	122	2
9	403	344	11.5	1.17	0.0546	0.0075	0.1254	0.0116	0.0195	0.0003	395	304	135	11	123	2
10	246	187	5.76	1.32	0.0545	0.0025	0.1242	0.0058	0.0193	0.0003	388	65	136	6	123	2
11	427	325	10.3	1.31	0.0544	0.0024	0.1243	0.0058	0.0193	0.0003	386	73	134	6	122	2
12	237	174	5.55	1.36	0.0462	0.00482	0.1262	0.0121	0.0188	0.00036	298	213	114	10	121	2
KJ01																
1	382	265	8.22	1.44	0.0463	0.0034	0.1186	0.0083	0.0189	0.0003	423	154	116	9	119	2
2	236	165	5.13	1.43	0.0462	0.0032	0.1213	0.0077	0.0192	0.0004	382	145	117	7	122	2
3	289	221	6.83	1.31	0.0463	0.0052	0.1189	0.0127	0.0186	0.0003	465	218	116	10	119	2
4	233	172	5.24	1.35	0.0462	0.0038	0.1211	0.0102	0.0192	0.0003	293	187	115	10	122	2
5	188	113	3.83	1.66	0.0491	0.0068	0.1255	0.0141	0.0188	0.0004	145	276	123	12	121	3
6	289	226	6.88	1.28	0.0475	0.0037	0.1251	0.0098	0.0193	0.0003	73	181	122	9	122	2
7	239	172	5.33	1.39	0.0483	0.0045	0.1262	0.0115	0.0191	0.0003	106	205	123	10	121	2
8	166	93	3.21	1.78	0.0524	0.0098	0.1261	0.0125	0.0191	0.0004	294	364	131	12	121	3
9	132	103	3.13	1.28	0.0518	0.0067	0.1275	0.0131	0.0195	0.0005	276	285	132	12	123	3
10	209	171	5.06	1.22	0.0525	0.0061	0.1241	0.0137	0.0188	0.0004	263	274	127	14	121	2
11	208	145	4.73	1.43	0.0473	0.0051	0.1267	0.0128	0.0195	0.0004	72	226	123	12	124	2
12	266	202	6.14	1.32	0.0505	0.0028	0.1234	0.0073	0.0193	0.0003	215	98	126	9	122	2
CN01																
1	352	258	8.16	1.36	0.0525	0.0045	0.1291	0.0072	0.0195	0.0003	303	197	135	10	124	2
2	375	149	6.46	2.52	0.0462	0.0034	0.1304	0.0087	0.0195	0.0003	426	155	116	8	124	2
3	435	308	9.68	1.41	0.0521	0.0024	0.1317	0.0059	0.0198	0.0003	282	72	133	8	126	2
4	621	482	14.5	1.29	0.0496	0.0021	0.1305	0.0053	0.0194	0.0002	171	68	125	6	125	2
5	243	103	4.26	2.36	0.0544	0.0107	0.1303	0.0076	0.0192	0.0004	386	398	135	10	123	3
6	455	391	11.6	1.16	0.0462	0.0028	0.1301	0.0075	0.0192	0.0002	265	142	115	8	122	2
7	3375	996	43.6	3.39	0.0526	0.0015	0.1311	0.0045	0.0194	0.0002	308	53	135	6	123	1
8	336	275	8.06	1.22	0.0508	0.0027	0.1319	0.0067	0.0194	0.0003	227	88	126	6	123	2
9	581	484	15.7	1.20	0.0516	0.0026	0.1311	0.0066	0.0198	0.0003	273	81	132	6	127	2
10	678	345	12.5	1.97	0.0532	0.0038	0.1301	0.0073	0.0196	0.0004	332	156	142	10	126	3
11	495	356	11.2	1.39	0.0462	0.0024	0.1305	0.0061	0.0192	0.0002	266	112	117	6	123	1
12	381	323	9.45	1.18	0.0509	0.0024	0.1308	0.0063	0.0196	0.0002	232	83	132	6	124	2
13	608	586	16.5	1.04	0.0497	0.0018	0.1306	0.0055	0.0196	0.0002	188	73	128	6	126	1

Table 2 Major element concentrations (wt%) for the mafic dykes from western Shandong Province

Sample No.	SJ1	SJ2	SJ3	SJ4	SJ5	SJ6	SJ7	SJ8	KJ1	KJ2	KJ3	KJ4	CN1	CN2	CN3	CN4
SiO_2	51.49	51.54	51.39	51.55	51.51	51.47	51.42	51.39	51.48	51.52	51.36	51.43	51.41	51.42	51.37	51.39
TiO_2	0.28	0.26	0.25	0.24	0.25	0.26	0.25	0.26	0.27	0.25	0.23	0.25	0.22	0.23	0.22	0.23
Al_2O_3	20.43	20.22	20.52	20.34	20.23	20.61	20.74	20.42	20.84	20.53	19.93	20.25	20.12	20.25	20.43	20.36
Fe_2O_3	3.98	3.76	4.03	4.05	4.07	4.31	3.95	3.88	3.85	3.98	4.32	4.66	4.62	4.65	4.58	4.65
FeO	4.36	4.38	4.41	4.15	4.43	4.35	4.23	4.41	4.36	4.35	4.21	4.23	4.16	4.16	4.17	4.13
MnO	0.18	0.21	0.17	0.19	0.21	0.18	0.18	0.16	0.18	0.19	0.17	0.15	0.13	0.12	0.15	0.16
MgO	4.27	4.13	3.96	3.95	4.02	4.15	3.97	3.86	3.86	3.92	4.26	4.43	4.38	4.33	4.25	4.18
CaO	5.46	5.57	6.04	5.61	5.53	5.38	5.36	5.35	5.38	5.42	5.38	5.43	5.35	5.32	5.35	5.34
Na_2O	3.62	3.76	3.69	3.83	3.73	3.63	3.57	3.54	3.62	3.59	3.48	3.54	3.47	3.51	3.48	3.46
K_2O	3.14	3.25	3.16	3.31	3.23	3.12	3.13	3.12	3.16	3.22	3.16	3.22	3.18	3.22	3.15	3.16
P_2O_5	0.23	0.26	0.21	0.24	0.25	0.22	0.21	0.22	0.22	0.23	0.24	0.23	0.22	0.21	0.22	0.21
LOI	2.12	2.34	1.98	2.23	2.36	2.21	2.25	2.62	2.15	2.12	2.46	1.65	2.14	1.92	1.95	2.17
Total	99.53	99.66	99.79	99.65	99.75	99.88	99.22	99.21	99.33	99.29	99.17	99.42	99.38	99.29	99.29	99.38
$Mg^{\#}$	49	49	47	47	47	47	48	47	47	47	48	48	48	48	48	47

Note: LOI = loss on ignition, $Mg^{\#} = 100(Mg/(Mg + Fe)$ in atomic proportions

Table 3 Trace element compositions ($\times 10^{-6}$) of the mafic dykes from western Shandong Province

Sample No.	SJ1	SJ2	SJ3	SJ4	SJ5	SJ6	SJ7	SJ8	KJ1	KJ2	KJ3	KJ4	CN1	CN2	CN3	CN4
Sc	25.2	26.3	24.8	26.4	25.5	24.9	24.8	25.2	22.9	21.8	23.5	23.4	28.3	29.5	30.6	29.2
V	246	245	236	247	253	239	246	248	285	286	269	281	186	193	196	212
Cr	143	146	136	154	138	143	146	141	54.1	46.3	65.2	73	375	383	373	387
Ni	38.9	37.6	36.4	36.7	38.2	38.1	38.4	38.5	24.8	18.8	26.3	27.2	93.2	95.6	89.1	96.3
Ga	22.3	21.4	21.7	20.7	22.1	21.4	20.9	21.6	22.2	25.6	23.5	24.6	18.6	18.7	18.8	18.6
Rb	71.5	63.9	54.8	62.8	69.5	63.6	63.9	70.8	62.8	69.6	65.7	67.6	58.4	59.4	57.8	59.6
Sr	871	824	816	816	866	825	832	858	952	938	966	975	706	712	703	716
Y	17.8	17.5	17.3	17.6	17.4	17.6	17.9	17.2	16.5	15.9	17.3	17.5	17.5	17.9	17.4	17.6
Zr	106	103	98.5	105	103	102	106	104	106	128	134	139	85.3	86.4	84.3	85.7
Nb	6.65	6.54	6.68	6.63	6.73	6.65	6.46	6.58	6.35	6.56	6.57	6.62	5.36	5.38	5.35	5.37
Ba	718	679	685	682	725	693	698	732	863	873	879	893	687	679	676	682
Hf	2.49	2.48	2.53	2.47	2.53	2.46	2.55	2.54	2.35	2.65	2.76	2.74	2.36	2.37	2.38	2.41
Ta	0.33	0.34	0.36	0.33	0.31	0.38	0.39	0.32	0.33	0.42	0.45	0.46	0.34	0.34	0.33	0.35
Pb	18.6	17.8	17.4	17.6	18.4	17.5	17.6	18.6	20.2	26.2	21.8	22.4	12.6	12.4	12.5	12.6
Th	5.43	5.38	5.29	5.35	5.39	5.42	5.37	5.34	6.12	7.23	6.27	6.34	4.46	4.48	4.45	4.49
U	1.52	1.51	1.48	1.54	1.51	1.46	1.48	1.54	1.66	2.03	1.78	1.83	1.35	1.36	1.34	1.36
La	32.1	31.6	31.7	31.8	32.2	31.6	31.4	32.5	24.5	26.3	25.7	25.5	21.2	21.4	21.3	21.2
Ce	72.3	66.7	65.4	65.6	67.1	66.2	71.5	65.9	50.2	61.5	56.3	56.5	48.3	49.5	48.2	49.8
Pr	7.76	6.65	6.73	6.58	7.57	6.71	6.73	7.49	5.75	7.16	5.89	5.95	5.92	5.96	5.87	5.85
Nd	33.5	34.2	33.7	35.1	34.5	34.3	34.5	34.8	25.3	27.2	25.8	26.2	25.7	25.9	25.4	25.3
Sm	6.35	6.31	6.42	6.34	6.34	5.98	5.83	6.35	4.78	5.81	5.16	5.18	5.08	4.95	5.06	5.03
Eu	1.65	1.63	1.64	1.65	1.63	1.64	1.63	1.65	1.37	1.53	1.37	1.37	1.36	1.36	1.37	1.36
Gd	4.89	5.06	4.95	5.05	4.74	4.84	4.66	4.76	3.88	4.66	4.25	4.26	4.23	4.26	4.18	4.25
Tb	0.66	0.72	0.68	0.75	0.64	0.73	0.76	0.64	0.56	0.65	0.62	0.64	0.58	0.57	0.56	0.56
Dy	3.91	3.94	3.78	3.76	4.02	3.74	3.69	4.04	2.96	3.54	3.33	3.29	3.28	3.27	3.29	3.18
Ho	0.72	0.73	0.71	0.68	0.68	0.69	0.66	0.69	0.56	0.68	0.64	0.63	0.58	0.62	0.61	0.61
Er	2.06	2.08	2.02	2.07	2.05	2.06	2.03	2.07	1.53	1.85	1.74	1.76	1.72	1.74	1.68	1.73
Tm	0.25	0.26	0.24	0.23	0.25	0.23	0.25	0.23	0.22	0.23	0.24	0.25	0.23	0.24	0.22	0.22
Yb	1.74	1.76	1.73	1.75	1.72	1.73	1.74	1.68	1.32	1.75	1.53	1.52	1.46	1.44	1.45	1.43
Lu	0.22	0.21	0.22	0.23	0.25	0.23	0.24	0.22	0.21	0.23	0.23	0.22	0.23	0.23	0.22	0.21
Eu/Eu^{*}	0.9	0.9	0.9	0.9	0.9	0.9	1	0.9	1	0.9	0.9	0.9	0.9	0.9	0.9	0.9

Notes: chondrite-normalisation factors for $(La/Yb)_N$ are from Sun and McDonough (1989); (Eu quantifies the anomalous behaviour of Eu in relation to the interpolated value for this element ((Sm + Gd)/2)

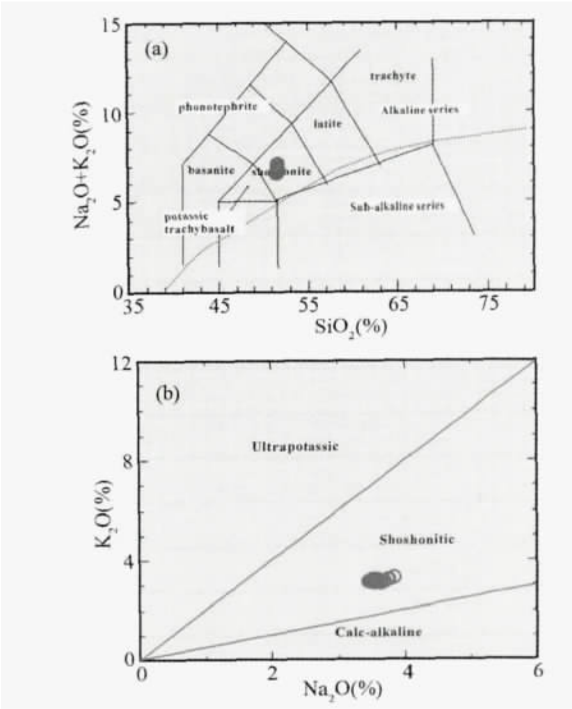

Fig. 3 Classification of the mafic dykes from western Shandong Province

(a) TAS diagram (after Middlemost, 1994; Le Maitre, 2002), where all major element concentrations are recalculated to 100% volatile-free compositions, and (b) Na_2O vs. K_2O diagram (after Menzies and Kyle, 1972)

and Sr. Mass fractionation corrections for Sr and Nd isotopic ratios were based on $^{86}Sr/^{88}Sr = 0.1194$ and $^{146}Nd/^{144}Nd = 0.7219$, respectively, and analysis of the NBS987 and La Jolla standards yielded values of $^{87}Sr/^{86}Sr = 0.710246 \pm 16$ (2sm), and $^{143}Nd/^{144}Nd = 0.511863 \pm 8$ (2sm), respectively.

3.4 In situ zircon Hf isotopic analysis

In situ zircon Hf isotopic analyses were conducted using a Neptune multiple collector-ICP-MS, equipped with a 193nm laser, at the Institute of Geology and Geophysics, Chinese Academy of Sciences, China. During the analyses, a laser repetition rate of 10Hz at 100mJ was used, and spot sizes were 32 and 63μm. Details of the analytical technique are described in Wu *et al.* (2006). During the analyses, the $^{176}Hf/^{177}Hf$ and $^{176}Lu/^{177}Hf$ ratios of the standard zircon 91500 were 0.282300 ± 15 (2sm, $n = 24$) and 0.00030, respectively, similar to the commonly accepted $^{176}Hf/^{177}Hf$ ratios of 0.282302 ± 8 and 0.282306 ± 8 (2sm) measured using the solution method (Goolaerts *et al.*, 2004).

4 Results

4.1 Zircon U-Pb ages

Euhedral zircon grains in samples SJ01, SJ01, KJ01 and CN01 are clean and prismatic, with magmatic oscillatory zoning (Fig. 2). A total of 13 grains provided a weighted mean $^{206}Pb/^{238}U$ age of 123.2 ± 0.6Ma (2σ) (95% confidence interval) for SJ01, 12 grains gave a weighted mean $^{206}Pb/^{238}U$ age of 122.0 ± 0.6Ma (2σ) (95% confidence interval) for SJ02, 12 grains gave a weighted mean $^{206}Pb/^{238}U$ age of 121.9 ± 0.6Ma (2σ) (95% confidence interval) for KJ01 (Table 1; Fig. 2a-d) and 13 grains gave a weighted mean $^{206}Pb/^{238}U$ age of 124.3 ± 0.5Ma (2σ) (95% confidence interval) for CN01. These weighted mean ages are the best estimates for the times of these doleritic dykes crystallised. Some inherited zircons were observed.

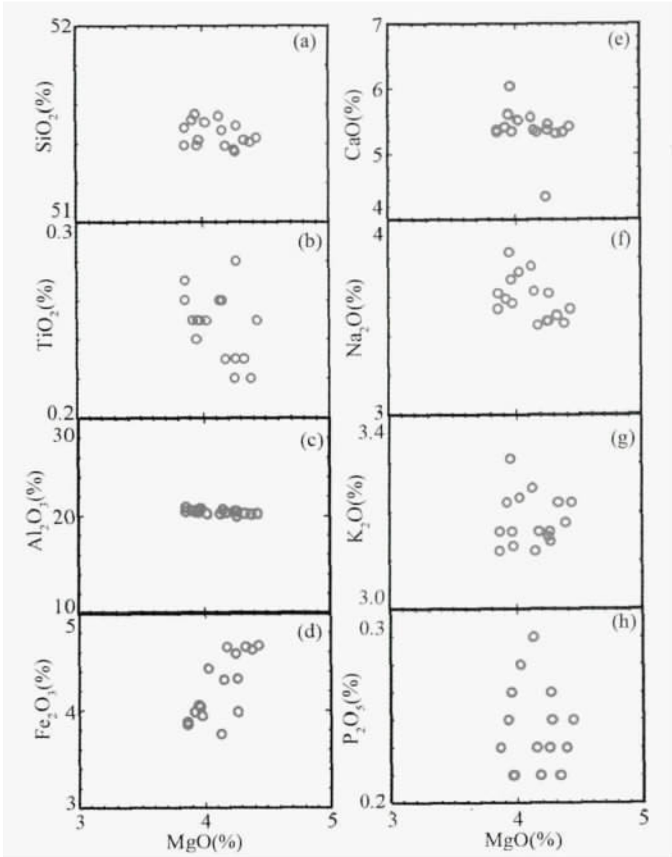

Fig. 4 Variations in major element contents compared with MgO for the mafic dykes of western Shandong Province

4.2 Major and trace element geochemistry

Geochemical data for the mafic dykes in the study area are presented in Tables 2 and Table 3. The diabase samples exhibit a narrow range of geochemical compositions, falling into the alkaline field when plotted on the total alkali-silica diagram (Fig. 3a); the rock type is phonotephrite. The mafic dyke samples also display an affinity to shoshonitic compositions in terms of Na_2O vs. K_2O (Fig. 3b). The dykes display obscure trends of decreasing TiO_2, Al_2O_3, K_2O, Na_2O and P_2O_5 with increasing MgO (Fig. 4b, c, f-h), and a positive correlation between Fe_2O_3 and MgO. They are also characterised by a relative enrichment in light rare earth elements, with a wide range of $(La/Yb)_N$ ratios (10.4 ~ 13.9) and negligible Eu anomalies ($Eu/Eu^* = 0.9 \sim 1.0$) (Table 3; Fig. 5a). On primitive-mantle-normalised trace element diagrams, the mafic dykes show enriched in large ion lithophile elements (i.e., Rb, Ba, U, K and Pb) and P, as well as depleted in high field strength elements (i.e., Nb, Ta and Ti) (Fig. 5b).

Table 4 Sr-Nd isotopic compositions of the mafic dykes from western Shandong Province

Sample No.	Age(Ma)	Rock type	$^{87}Rb/^{86}Sr$	$^{87}Sr/^{86}Sr$	2sm	$(^{87}Sr/^{86}Sr)_i$	$^{147}Sm/^{144}Nd$	$^{143}Nd/^{144}Nd$	2sm	$(^{143}Nd/^{144}Nd)_i$	$\varepsilon_{Nd}(t)$
SJ1	123.2	Dolerite	0.238	0.710208	5	0.709782	0.1141	0.511828	10	0.511736	-14.5
SJ3			0.194	0.710133	6	0.709793	0.1147	0.511824	10	0.511732	-14.6
SJ4			0.223	0.710182	6	0.709782	0.1087	0.511821	9	0.511733	-14.6
SJ5	122.0		0.283	0.710285	6	0.709785	0.1373	0.511842	10	0.511732	-14.6
SJ8			0.337	0.710381	8	0.709796	0.1405	0.511838	9	0.511726	-14.7
KJ1	121.9		0.391	0.710473	6	0.709806	0.1384	0.511845	9	0.511735	-14.6
KJ2			0.337	0.710379	5	0.709785	0.1282	0.511842	9	0.511740	-14.5
CN2	124.3		0.631	0.710912	8	0.709797	0.1294	0.511836	10	0.511731	-14.6
CN3			0.610	0.710873	6	0.709786	0.1316	0.511831	12	0.511724	-14.7
CN4			0.629	0.710906	8	0.709785	0.1296	0.511837	10	0.511733	-14.5

Note: the Chondrite Uniform Reservoir values and decay constants of $\lambda_{Rb} = 1.42 \times 10^{-11}$ year^{-1} (Steiger and Jäger, 1977) and $\lambda_{Sm} = 6.54 \times 10^{-12}$ year^{-1} (Lugmair and Harti, 1978)

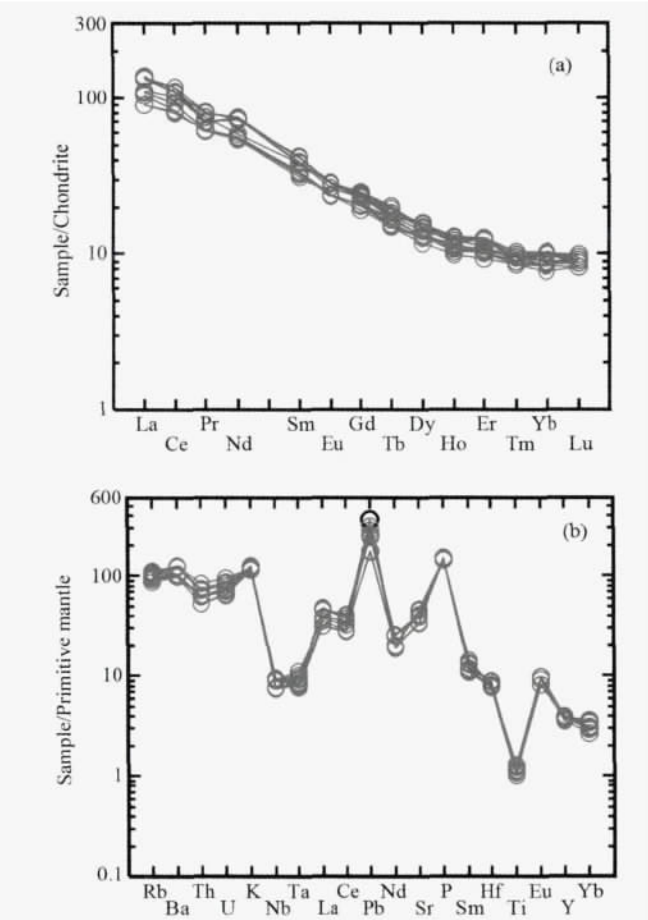

Fig. 5 Chondrite-normalized rare earth element patterns (a) and primitive-mantle-normalized incompatible element distribution diagrams (b) for the mafic dykes of western Shandong Province (normalization values after Sun and McDonough, 1989)

4.3 Sr-Nd isotopes

Sr-Nd isotopic data were obtained for 10 representative mafic dyke samples (Table 4). The dykes show uniform $(^{87}Sr/^{86}Sr)_i$ values (~0.7098) and little variation in $\varepsilon_{Nd}(t)$ values (from -14.7 to -14.5). The Sr-Nd isotopic compositions (Fig. 6) are comparable to those of Mesozoic mafic rocks from the Sulu Belt (Li *et al.*, 1998; Jahn *et al.*, 1999; Fan *et al.*, 2004; Wang *et al.*, 2005) and Shandong Province (Liu, 2004; Liu *et al.*, 2008a, b, 2009a). However, they differ from those of Mesozoic mafic dykes in the Yangtze Craton (Chen *et al.*, 2001; Li *et al.*, 2004) and other parts of the North China Craton (Guo *et al.*, 2001).

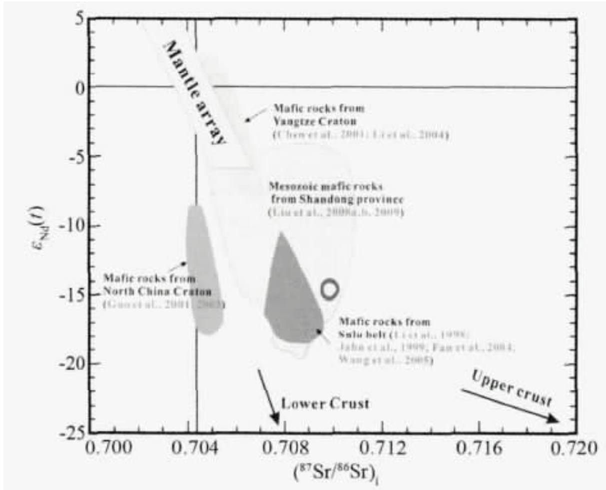

Fig. 6 Variations in initial $^{87}Sr/^{86}Sr$ vs. $\varepsilon_{Nd}(t)$ values for the mafic dykes of western Shandong Province

Also shown is a field delineating the composition of Mesozoic mafic dykes within the Yangtze Craton, NCC, the Sulu Belt and other areas in Shandong Province (Li *et al.*, 1998, 2004; Jahn *et al.*, 1999; Chen *et al.*, 2001; Guo *et al.*, 2001; Fan *et al.*, 2004; Liu, 2004; Wang *et al.*, 2005; Liu *et al.*, 2008a, b, 2009a). The mafic dykes analysed during this study plot within the field of an enriched mantle source

4.4 Zircon Hf isotopes

Four samples of zircon dated by LA-ICP-MS zircon U-Pb dating were also analysed for their Lu-Hf isotopes, and the results are presented in Table 5. Fifteen spot analyses were performed on zircon from sample KJ01. The determined negative $\varepsilon_{Hf}(t)$ values for this dyke vary between -30.4 and -28.6

Table 5 Zircon Lu-Hf isotopic compositions of the mafic dykes from Shandong Province

Spot No.	Age(Ma)	$^{176}Yb/^{177}Hf$	2sm	$^{176}Lu/^{177}Hf$	2sm	$^{176}Hf/^{177}Hf$	2sm	$\varepsilon_{Hf}(t)$	t_{DM1}(Ma)	$f_{Lu/Hf}$
KJ01										
1		0.0258	0.010990	0.000656	0.000047	0.281858	0.000016	−29.7	1941	−0.98
2		0.0255	0.010640	0.000613	0.000034	0.281865	0.000015	−29.5	1930	−0.98
3		0.0386	0.015845	0.000944	0.000054	0.281896	0.000014	−28.4	1904	−0.97
4		0.0175	0.007112	0.000424	0.000024	0.281844	0.000015	−30.2	1950	−0.98
5		0.0149	0.005954	0.000370	0.000019	0.281839	0.000014	−30.4	1954	−0.96
6		0.0179	0.007031	0.000428	0.000022	0.281886	0.000016	−28.7	1892	−0.97
7		0.0254	0.009835	0.000656	0.000033	0.281875	0.000017	−29.1	1919	−0.98
8	121.9	0.0323	0.012428	0.000778	0.000056	0.281876	0.000015	−29.1	1923	−0.98
9		0.0185	0.006966	0.000443	0.000021	0.281869	0.000016	−29.3	1917	−0.95
10		0.0319	0.011939	0.000760	0.000044	0.281857	0.000015	−29.8	1949	−0.98
11		0.0385	0.014082	0.000903	0.000044	0.281847	0.000013	−30.1	1969	−0.97
12		0.0359	0.012916	0.000871	0.000040	0.281842	0.000015	−30.3	1975	−0.97
13		0.0125	0.004418	0.000313	0.000014	0.281867	0.000014	−29.4	1913	−0.95
14		0.0296	0.010330	0.000765	0.000040	0.281841	0.000016	−30.3	1971	−0.98
15		0.0308	0.010567	0.000722	0.000032	0.281889	0.000018	−28.6	1903	−0.98
SJ02										
1		0.0615	0.000961	0.001945	0.000037	0.281871	0.000011	−29.4	1991	−0.95
2		0.0603	0.002117	0.001666	0.000059	0.281888	0.000014	−28.7	1952	−0.95
3		0.0577	0.001382	0.001502	0.000027	0.281871	0.000013	−29.3	1968	−0.95
4		0.0215	0.000917	0.000582	0.000025	0.281892	0.000010	−28.5	1891	−0.98
5		0.0517	0.002365	0.001379	0.000067	0.281875	0.000013	−29.2	1955	−0.96
6		0.0599	0.002088	0.001559	0.000056	0.281887	0.000013	−28.8	1948	−0.95
7		0.0240	0.000298	0.000633	0.000003	0.281864	0.000011	−29.5	1932	−0.98
8	122.0	0.0358	0.000526	0.000976	0.000015	0.281885	0.000012	−28.8	1832	−0.97
9		0.0489	0.001561	0.001226	0.000038	0.281880	0.000017	−29.0	1918	−0.96
10		0.0404	0.000614	0.001110	0.000019	0.281890	0.000014	−28.6	1902	−0.97
11		0.0458	0.002071	0.001172	0.000053	0.281896	0.000014	−28.4	1994	−0.96
12		0.0409	0.000818	0.001097	0.000015	0.281889	0.000014	−28.6	1888	−0.97
13		0.0375	0.000522	0.001034	0.000013	0.281886	0.000013	−28.7	1817	−0.97
14		0.0432	0.000586	0.001139	0.000014	0.281875	0.000016	−29.1	1943	−0.97
15		0.0741	0.003640	0.002021	0.000106	0.281898	0.000013	−28.4	1957	−0.95
SJ01										
1		0.0128	0.000961	0.000334	0.000037	0.281808	0.000011	−31.4	1994	−0.95
2		0.0347	0.002117	0.001047	0.000059	0.281833	0.000014	−30.6	1997	−0.95
3		0.0613	0.001382	0.001463	0.000027	0.281902	0.000013	−28.2	1922	−0.98
4		0.0488	0.000917	0.001218	0.000025	0.281864	0.000010	−29.5	1962	−0.96
5		0.0765	0.002365	0.001924	0.000067	0.281921	0.000013	−27.6	1919	−0.95
6		0.0198	0.002088	0.000495	0.000056	0.281835	0.000013	−30.5	1965	−0.98
7		0.0603	0.000298	0.001666	0.000003	0.281837	0.000011	−30.5	2024	−0.97
8	123.2	0.0577	0.000526	0.001502	0.000015	0.281841	0.000012	−30.4	2010	−0.98
9		0.0215	0.002787	0.000582	0.000069	0.281833	0.000012	−30.6	1973	−0.95
10		0.0517	0.001021	0.001379	0.000056	0.281831	0.000013	−30.7	2017	−0.96
11		0.0599	0.001416	0.001559	0.000035	0.281842	0.000019	−30.3	2011	−0.96
12		0.0240	0.001416	0.000633	0.000035	0.281844	0.000019	−30.2	1960	−0.96
13		0.0358	0.001561	0.000976	0.000038	0.281901	0.000017	−28.2	1898	−0.97
14		0.0432	0.000614	0.001139	0.000019	0.281862	0.000014	−29.6	1961	−0.96
15		0.0375	0.002071	0.001034	0.000053	0.281858	0.000013	−29.7	1961	−0.97
CN01										
1		0.0392	0.000436	0.000998	0.000017	0.281842	0.000014	−30.3	1982	−0.97
2		0.0290	0.000581	0.000723	0.000011	0.281867	0.000013	−29.3	1933	−0.98
3		0.0350	0.001260	0.000857	0.000028	0.281869	0.000014	−29.3	1937	−0.97
4		0.0294	0.000425	0.000719	0.000012	0.281896	0.000014	−28.3	1893	−0.98
5		0.0447	0.002259	0.001121	0.000055	0.281954	0.000020	−26.3	1833	−0.97
6		0.0475	0.000437	0.001190	0.000015	0.281892	0.000013	−28.5	1922	−0.96
7		0.0340	0.000512	0.000830	0.000008	0.281893	0.000014	−28.5	1903	−0.97
8	124.3	0.0148	0.000342	0.000397	0.000005	0.281870	0.000012	−29.2	1912	−0.96
9		0.0316	0.000599	0.000787	0.000011	0.281896	0.000012	−28.3	1896	−0.98
10		0.0211	0.000393	0.000532	0.000008	0.281893	0.000012	−28.4	1888	−0.98
11		0.0284	0.000520	0.000709	0.000016	0.281879	0.000013	−28.9	1916	−0.95
12		0.0320	0.000376	0.000767	0.000012	0.281891	0.000014	−28.5	1902	−0.98
13		0.0388	0.001194	0.000934	0.000021	0.281859	0.000012	−29.6	1954	−0.97
14		0.0404	0.002140	0.000968	0.000053	0.281900	0.000017	−28.2	1900	−0.97
15		0.0271	0.000260	0.000675	0.000006	0.281895	0.000013	−28.4	1892	−0.98

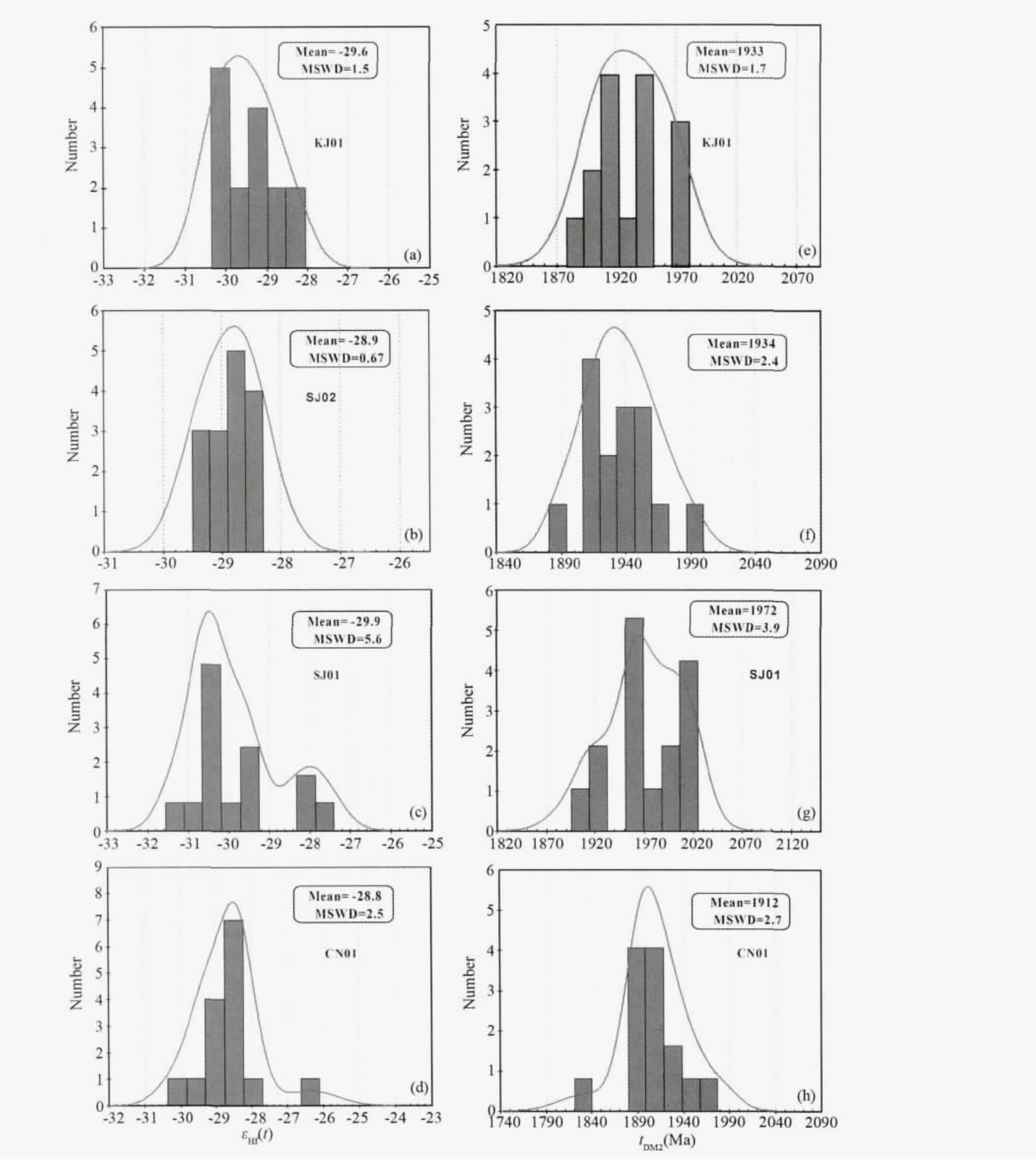

Fig. 7 Histograms of zircon $\varepsilon_{Hf}(t)$ values (a-d) and two-stage Hf model ages (e-h) for the mafic dykes in western Shandong Province

(Table 5; Fig. 7a). This sample has initial $^{176}Hf/^{177}Hf$ ratios that vary between 0.281839 and 0.281896. Fifteen spot analyses were made for sample SJ02. The determined negative $\varepsilon_{Hf}(t)$ values for this zircon vary between −29.5 and −28.4 (Table 5; Fig. 7b). This sample has initial $^{176}Hf/^{177}Hf$ ratios that vary between 0.281864 and 0.281898. Fifteen spot analyses were obtained for zircon sample SJ01, yielding variable $\varepsilon_{Hf}(t)$ values between −31.4 and −27.6 (Table 5; Fig. 7c), and giving initial $^{176}Hf/^{177}Hf$ ratios ranging from 0.281808 to 0.281921. Fifteen spot analyses were obtained for zircon sample SJ01, yielding variable $\varepsilon_{Hf}(t)$ values between −30.3 and −26.7 (Table 5; Fig. 7d), and initial $^{176}Hf/^{177}Hf$ ratios ranging from

0.281842 to 0.281896.

5 Petrogenesis

5.1 Lithospheric mantle source

The investigated Early Cretaceous mafic dykes are characterised by low SiO_2 contents (51.4% ~ 51.5%; Table 2), suggesting they were derived from an ultramafic source (Liu *et al.*, 2008a, b, 2009a, 2013a, b, c, d). Crustal rocks can be ruled out as possible sources, as partial melting of any of the crustal rocks (e.g., Hirajima *et al.*, 1990) and lower crustal intermediate granulites (Gao *et al.*, 1998) in the deep crust would produce liquids with high Si and low Mg contents (i.e., granitoid liquids; Rapp *et al.*, 2003). The high initial $^{87}Sr/^{86}Sr$ ratios (~0.7098), negative $\varepsilon_{Nd}(t)$ values (−14.7 to −14.5) and zircon $\varepsilon_{Hf}(t)$ values (−31.4 to −26.7) (Tables 4 and Table 5) for the mafic dykes are consistent with derivation from an enriched lithospheric mantle source rather than an asthenospheric mantle source with a depleted Sr-Nd isotopic composition, such as Middle Ocean Ridge Basalt (MORB).

5.2 Crustal contamination

Crustal contamination might cause a significant depletion in Nb-Ta and enriched Sr-Nd isotopic signatures in basaltic rocks (Guo *et al.*, 2004). The dolerites studied here are characterised by negative Nb-Ta anomalies (Table 3; Fig. 5b), and this implies a crustal component in the genesis of the mafic dyke magma. In Fig. 4a, b, e and h, the major elements such as SiO_2, CaO, TiO_2, and P_2O_5 and so on actually show obscure linear correlation with MgO. This would suggest that magma mixing or contamination might have played an important role during the magma ascending. The above observation is further supported by inherited zircons, the fact that the dykes have low Ni (18.8×10^{-6} ~ 96.3×10^{-6}) (Table 3), no correlation between $Mg^{\#}$, Ni and initial Sr ratio (not shown), distinctive negative high field strength elements (Nb, Ta, and Ti), positive Pb anomalies (Fig. 5a, b; Zhang *et al.*, 2005), and high Ba/Nb ratios (103 ~ 136; Table 3; Jahn *et al.*, 1999).

5.3 Genetic model

All of the mafic dykes studied here have similar characteristics in terms of their geochemistry and isotopes, implying a similar source region. On a plot of La versus La/Sm (not shown), all the samples are distributed along a trend line for partial melting, indicating the dykes were derived by partial melting of an enriched mantle. In addition, as noted above, the possibility of significant and direct assimilation of crust during the genesis of the mafic magmas occurred. Moreover, in the primitive-mantle-normalised diagram (Fig. 5b), all the dykes show distinctive negative anomalies in Nb, Ta and Ti, and positive anomalies in Pb. HFSE-depletion could indicate the involvement of components from the proto-Tethyan oceanic or ancient continental crust (Zhang *et al.*, 2005). In addition, the higher La/Nb (3.9 ~ 4.9) and Ba/Nb ratios (103 ~ 135) in these rocks (Table 3) differ from those of most intraplate volcanic rocks, including Ocean Island Basalt (OIB), alkali basalt and kimberlite, which have much lower ratios of La/Nb (2.5 ~ 0.5) and Ba/Nb (20 to 1) (Jahn *et al.*, 1999). These data suggest that continental materials (granitoids, granulites, sediments etc.) were involved in the petrogenesis of the mantle-derived magmas, which is further supported by the low $\varepsilon_{Nd}(t)$ values from −14.7 to −14.5 and high $(^{87}Sr/^{86}Sr)_i$ values (~0.7098) (Table 4; Fig. 6). Therefore, we propose the involvement of crustal components that were already incorporated into the mantle source. Nevertheless, it is necessary to know by which mechanism those crustal materials may have been incorporated.

Accordingly, a genetic model is required to decipher the origin of these dykes. At present, at least two competing mechanisms can be envisaged (Liu *et al.*, 2008a, b, c, 2009a, 2013b): (1) contributions from the subducting Yangtze Block, and (2) the action of the subducted ancient Pacific Plate (Cai *et al.*, 2013; Tang *et al.*, 2013). However, it is generally believed that the final collision between the NCC and the Yangtze Block occurred during the Triassic (Meng and Zhang, 1999; Zhang *et al.*, 2005), and there was no westwards subduction of an ancient Pacific Plate below the NCC before the Early Cretaceous (Xu *et al.*, 1993). Furthermore, no evidence has yet been presented that a contribution of the Palaeo-Pacific Plate to Mesozoic magmatism in the eastern NCC (Zhang *et al.*, 2005). Thus, it is unlikely that the petrogenesis of these magmas relates to either a subducting Yangtze lithosphere or ancient Pacific Plate. An alternative model, therefore, is required to account for how the mafic dykes were formed.

Since the direct assimilation of crustal material has been shown to be negligible in the genesis of the mafic dykes in the Zichuan area, and if the role of subducting lithosphere (either the Yangtze or Palaeo-Pacific plates) can been discounted, it is necessary to know by which reasonable mechanism crustal materials may have been incorporated into the underlying lithospheric mantle. The foundering of the lower continental crust has been suggested as a possible genetic model for the origin of the Mesozoic mafic dykes in Shandong Province (Liu *et al.*, 2008a, b, 2009a, b), and because of its higher density than lithospheric mantle (Anderson, 2006), eclogite can be recycled into the mantle (Kay and Mahlburg-Kay, 1991; Jull and Kelemen, 2001; Gao *et al.*, 2004). Moreover, eclogites have lower melting temperatures than mantle peridotites (Yaxley, 2000; Kogiso *et al.*, 2003), and so foundered. Silica-saturated eclogite may partially melt to produce silicic melts (tonalite to trondhjemite) that may be hybridised with the overlying mantle peridotite. Such hybridisation could produce an olivine-free pyroxenite, which, if subsequently melted, would generate basaltic melt (Kogiso *et al.*, 2003; Herzberg *et al.*, 2007; Gao *et al.*, 2008). In the eastern NCC, this model is further supported by observations of intensive lithospheric thinning (Liu *et al.*, 2008a, b), voluminous coeval magmatism (130 ~ 120Ma) (Wang *et al.*, 1998; Guo *et al.*, 2001; Yang *et al.*, 2003, 2004; Liu *et al.*, 2004, 2008a, b, c; Zhang *et al.*, 2004; Li *et al.*, 2013), large-scale mineralization (Wang *et al.*, 1998; Yang *et al.*, 2003, 2004) and the presence of adakitic rocks (Gao *et al.*, 2004; Liu *et al.*, 2008c, 2009b), all of which could be produced during a process of lithospheric foundering.

Nevertheless, if delamination of eclogitic lower crust occurred, this would lead to rapid uplift of the study area (Menzies *et al.*, 2007). Evidence for this uplift is lacking, however. At the same time, lithospheric delamination would induce asthenospheric upwelling, leading to decompression melting and the formation and eruption of basalt with similar geochemical features to that of MORB or OIB. The absence of such asthenospherically-derived magma contemporaneous with the studied dykes thus argues against a delamination of the lithosphere. Moreover, the study dykes are characterized by depletion in Th and U, and enrichment in K; they all exclude the possibility of delamination of lower crust. Thus, what is the cause of the enriched mantle source to the mafic magmas, and where do the hybridized materials derive? These key issues will be discussed next.

By contrast with the exposed Archaean-Proterozoic metamorphic complexes and typical marine sediment as a possible explanation, Guo *et al.* (2014) sought help from 'cold' subduction of the Yangtze Craton to explain the origin of the mafic dykes (115Ma) from Jiaodong peninsula. Their interpretation has provided credible evidence, based on which, we propose that a sedimentary component derived from Yangtze Craton, continental crust to be the cause of mantle enrichment beneath the study area. The interaction of sedimentary melt with overlying mantle lithologies helped to generate fertile mantle pyroxenite. Partial melting of this modified, and olivine-poor, pyroxenite can produce Mg-rich magmas with low Nb-Ta-Ti concentrations. In the Guo *et al.* (2014) study, it was indeed suggested that fertile pyroxenite, formed through sediment melt–peridotite interaction, to be the source of mafic dykes emplaced along the western Shandong Province (Guo *et al.*, 2014). In accordance with geophysical observations (Engebretson *et al.*, 1985), oblique subduction of the paleo-Pacific Plate towards the NCC occurred during the Early Cretaceous. This subduction exerted a driving force to induce the extensive collapse of the southeastern margin of the NCC, triggering extensive melting of the metasomatized mantle responsible for mafic magmatism across the NCC (Wu *et al.*, 2005).

As such, a special model can explain the formation of the mafic dykes within the sutdy area. Chemenda *et al.* (2000) proposed a two-dimensional thermo-mechanical, laboratory model for continental subduction, and used this to interpret the evolutionary history of the India-Asia collisional system. They suggested that subducted continental crust or sediments would be detached from underlying lithosphere mantle if the subduction was sufficiently rapid or if the subducted lithosphere had a thick lower crust (Zhang and Sun, 2002). This model may be suitable for the Triassic, Dabie collisional zone because the Yangtze Craton is an old Craton and should have had a thickened lower crust. Thus, we adopt this explanation to help reconstruct possible scenarios for the Dabie collision and for the formation of the Mesozoic lithosphere adjacent to the Dabie Orogen.

At ~240Ma, collision between the Yangtze Craton and the NCC occurred along with northward subduction of the paleo-Tethys oceanic lithosphere (Zhang and Sun, 2002). The Yangtze lithosphere was dragged down into mantle by the denser oceanic lithosphere it comprised. Subsequently, the upper/middle Yangtze crust and sedimentary drape reached a depth of ~200km (Ye *et al.*, 2000; Zhang and Sun, 2002) and subsequently rapidly moved upward between the NCC and Yangtze Craton in response to slab break-off of the subducting oceanic lithosphere (Davies and Von Blanckenburgh, 1995; O'Brien, 2001). At ~220Ma, Yangtze subduction switched to a highly compressional mode (Chemenda *et al.*, 2000), which resulted in the detachment of the Yangtze crust and sediments from the mantle. The crust would be then tectonically underplated beneath the base of the NCC lithosphere because of its buoyancy relative to the surrounding mantle. This process would lead to a thickened continental root and an isostatic uplift of the southeastern NCC. The thickened continental root was then probably eclogitized (Leech, 2001) or melted (Skjerlie and Douge, 2002) by underlying asthenosphere.

Subsequently, silicic melts produced by melting of these crustal materials migrated through the overriding continental lithosphere and interacted with mantle peridotite. Extensive interaction would have completely destroyed the old lithosphere regime, finally generating the Sr-Nd isotopic enriched (hybridized) Mesozoic lithosphere that was the source for the Cretaceous dykes' intrusion. As a result, decompression melting of this enriched mantle at 125 ~ 120Ma produced primary basaltic melts that evolved to form the mafic magmas that were emplaced as swarms of dykes across the western Shandong Province of the southeastern NCC.

6 Conclusions

Based on new geochronological, geochemical and Sr-Nd and Hf isotopic studies of mafic dykes from the Zichuan area of western Shandong Province, the following conclusions can be drawn:

(1) U-Pb zircon dating indicates that the mafic dykes in western Shandong Province were emplaced between 121.9 ± 0.6Ma and 124.3 ± 0.5Ma.

(2) The mafic dykes in the study area are alkaline and shoshonitic, have high light rare earth element concentrations with slight negative Eu anomalies ((Eu = 0.9 ~ 1.0), and have positive Ba, K, Pb and P, and negative Nb, Ta, and Ti anomalies. These dykes were derived from partial melting of an enriched mantle source (($^{87}Sr/^{86}Sr)_i$ values = ~0.7098, $\varepsilon_{Nd}(t)$ values = −14.7 to −14.5), and formed from parental magmas that were generated during lithospheric extension-related partial melting of an enriched region of the lithospheric mantle beneath the southeastern NCC. In addition, there underwent significant contamination of these magmas during emplacement.

(3) The mafic dykes in the study area formed in an extensional setting following collision between the NCC and the Yangtze Craton. The magmas that formed these dykes were sourced from a hybridized source caused by subduction of Yangtze crustal sedimentary material beneath southeastern NCC before the Late Mesozoic.

Acknowledgements The authors thank Lian Zhou and Zhaochu Hu for assistance during zircon U-Pb dating and during analyses of Sr-Nd and Hf isotopes.

References

Andersen T. 2002. Correction of common lead in U-Pb analyses that do not report ^{204}Pb. Chemical Geology, 192(1–2): 59–79

Anderson DL. 2006. Speculations on the nature and cause of mantle heterogeneity. Tectonophysics, 416(1–4): 7–22

Cai YC, Fan HR, Santosh M, Liu X, Hu FF, Yang KF, Lan TG, Yang

YH and Liu YS. 2013. Evolution of the lithospheric mantle beneath the southeastern North China Craton: Constraints from mafic dikes in the Jiaobei terrain. Gondwana Research, 24(2): 601 - 621
Cao JJ. 2007. The geochemistry of Cenozoic mafic dykes from Guangdong and Hainan provinces, as well as lithosphere evolution. Ph. D. Dissertation. Guiyang: Institute of Geochemistry, Chinese Academy of Sciences (in Chinese)
Chemenda AI, Burg JP and Mattauer M. 2000. Evolutionary model of the Himalaya-Tibet system, Geopoem: Based on new modelling, geological and geophysical data. Earth and Planetary Science Letters, 174(3 - 4): 397 - 409
Chen H, Xia QK and Ingrin J. 2015. Water content of the Xiaogulihe ultrapotassic volcanic rocks, NE China: Implications for the source of the potassium-rich component. Science Bulletin, 60(16): 1468 - 1470
Chen JF, Yan J, Xie Z, Xu X and Xing FM. 2001. Nd and Sr isotopic compositions of igneous rocks from the Lower Yangtze region in eastern China: Constraints on sources. Physics and Chemistry of the Earth, Part A: Solid Earth and Geodesy, 26(9 - 10): 719 - 731
Chen XD and Shi LB. 1983. Primary research on the diabase dyke swarms in Wutai-Taihang area. Chinese Science Bulletin, 16: 1002 - 1005
Chen XD, Shi LB and Jia SF. 1992. Study of the Proterozoic dike swarm in North China. Seismology and Geology, 14(4): 351 - 357 (in Chinese with an English abstract)
Chen XD and Shi LB. 1994. Basic dyke swarms in extensional structures. In: Qian XL (ed.). Extensional Structures. Beijing: Geological Publishing House, 71 - 74
Davies JH and Von Blanckenburg F. 1995. Slab breakoff: A model of lithosphere detachment and its test in the magmatism and deformation of collisional orogens. Earth and Planetary Science Letters, 129(1 - 4): 85 - 102
Engebretson DC, Cox A and Gordon RG. 1985. Relative motions between oceanic and continental plates in the Pacific basin. GSA Special Paper, 206: 1 - 60
Ernst RE and Baragar WRA. 1992. Evidence from magnetic fabric for the flow pattern of magma in the Mackenzie giant radiating dyke swarm. Nature, 356(6369): 511 - 513
Ernst RE, Buchan KL and Palmer HC. 1995. The global mafic dykes Gis-Database project. Trans-Hudson Orogen Transect Lithoprobe Report, 38: 42 - 46
Ernst RE, Buchan KL and Campbell IH. 2005. Frontiers in large igneous province research. Lithos, 79(3 - 4): 271 - 297
Fan WM, Guo F, Wang YJ and Zhang M. 2004. Late Mesozoic volcanism in the northern Huaiyang tectono-magmatic belt, central China: Partial melts from a lithospheric mantle with subducted continental crust relicts beneath the Dabie orogen? Chemical Geology, 209(1 - 2): 27 - 48
Féraud G, Giannerini G and Campredon R. 1987. Dyke swarms as paleostress indicators in areas adjacent to continental collision zones: Examples from the European and Northwest Arabian Plates. In: Halls HC and Fahrig WF (eds.). Mafic Dyke Swarms. Geological Association of Canada Special Paper, 34: 273 - 278
Gao S, Zhang BR, Jin ZM, Kern H, Luo TC and Zhao ZD. 1998. How mafic is the lower continental crust? Earth and Planetary Science Letters, 106(1 - 4): 101 - 117
Gao S, Rudnick RL, Yuan HL, Liu XM, Liu YS, Xu WL, Ling WL, Ayers J, Wang XC and Wang QH. 2004. Recycling lower continental crust in the North China craton. Nature, 432(7019): 892 - 897
Gao S, Rudnick RL, Xu WL, Yuan HL, Liu YS, Walker RJ, Puchtel IS, Liu XM, Huang H, Wang XR and Yang J. 2008. Recycling deep cratonic lithosphere and generation of intraplate magmatism in the North China Craton. Earth and Planetary Science Letters, 270(1 - 2): 41 - 53
Goolaerts A, Mattielli N, de Jong J, Weis D and Scoates JS. 2004. Hf and Lu isotopic reference values for the zircon standard 91500 by MC-ICP-MS. Chemical Geology, 206(1 - 2): 1 - 9
Gudmundsson A. 1995. Infrastructure and mechanics of volcanic systems in Iceland. Journal of Volcanology and Geothermal Research, 64(1 - 2): 1 - 22
Guo F, Fan WM, Wang YJ and Lin G. 2001. Late Mesozoic mafic intrusive complexes in North China block: Constraints on the nature of subcontinental lithospheric mantle. Physics and Chemistry of the Earth, Part A: Solid Earth and Geodesy, 26(9 - 10): 759 - 771
Guo F, Fan WM, Wang YJ and Zhang M. 2004. Origin of Early Cretaceous calc-alkaline lamprophyres from the Sulu orogen in eastern China: Implications for enrichment processes beneath continental collisional belt. Lithos, 78(3): 291 - 305
Guo F, Fan WM, Li CW, Wang CY, Li HX, Zhao L and Li JY. 2014. Hf-Nd-O isotopic evidence for melting of recycled sediments beneath the Sulu Orogen, North China. Chemical Geology, 381: 243 - 258
Guo JH, Sun M, Chen FK and Zhai MG. 2005. Sm-Nd and SHRIMP U-Pb zircon geochronology of high-pressure granulites in the Sanggan area, North China Craton: Timing of Paleoproterozoic continental collision. Journal of Asian Earth Sciences, 24(5): 629 - 642
Halls HC. 1982. The importance and potential of mafic dyke swarms in studies of geodynamic processes. Geosciences Canada, 9(3): 145 - 154
Halls HC and Fahrig WF. 1987. Mafic dyke swarms. Geol. Assoc. Can. Spec. Paper, 34: 1 - 503
Halls HC and Hatts MP. 1990. Paleomagnetism of Proterozoic mafic dyke swarms of the Canadian Shield. In: Parker AJ, Rickwood PC and Tucker DH (eds.). Mafic Dykes and Emplacement Mechanisms: International Dykes Conference. Rotterdam: A. A. Balkema, 209 - 230
Herzberg C, Asimow PD, Arndt N, Niu Y, Lesher CM, Fitton JG, Cheadle MJ and Saunders AD. 2007. Temperatures in ambient mantle and plumes: Constraints from basalts, picrites, and komatiites. Geochemistry, Geophysics, Geosystems, 8(2): doi: 10.1029/2006GC001390
Hirajima T, Ishiwatari A, Cong B, Zhang R, Banno S and Nozaka T. 1990. Coesite from Mengzhong eclogite at Dhonghai County, northeastern Jiangsu Province, China. Mineralogical Magazine, 54(377): 579 - 583
Hou GT, Liu YL and Li JH. 2006. Evidence for ~1.8Ga extension of the Eastern Block of the North China Craton from SHRIMP U-Pb dating of mafic dyke swarms in Shandong Province. Journal of Asian Earth Sciences, 27(4): 392 - 401
Huang ZX, Li HY, Zheng YJ and Peng YJ. 2009. The lithosphere of North China Craton from surface wave tomography. Earth and Planetary Science Letters, 288(1 - 2): 164 - 173
Jahn BM, Wu FY, Lo CH and Tsai CH. 1999. Crust-mantle interaction induced by deep subduction of the continental crust: Geochemical and Sr-Nd isotopic evidence from post-collisional mafic-ultramafic intrusions of the northern Dabie complex, central China. Chemical Geology, 157(1 - 2): 119 - 146
Jull M and Kelemen PB. 2001. On the conditions for lower crustal convective instability. Journal of Geophysical Research, 106(B4): 6423 - 6446
Kay RW and Mahlburg-Kay S. 1991. Creation and destruction of lower continental crust. Geologische Rundschau, 80(2): 259 - 278
Kogiso T, Hirschmannmm and Frost DJ. 2003. High-pressure partial melting of garnet pyroxenite: Possible mafic lithologies in the source of ocean island basalts. Earth and Planetary Science Letters, 216(4): 603 - 617
Le Maitre RW. 2002. Igneous Rocks: A Classification and Glossary of Terms. 2nd Edition. Cambridge: Cambridge University Press, 1 - 236
Leech ML. 2001. Arrested orogenic development: Eclogitization, delamination, and tectonic collapse. Earth and Planetary Science Letters, 185(1 - 2): 149 - 159
Li CW, Guo F and Li XY. 2004. Petrogenesis and geodynamic implications of Late Mesozoic mafic volcanic rocks from the Lishui Basin of the Lower Yangtze region. Geochimica, 33(4): 361 - 371 (in Chinese with English abstract)

Li SG, Huang F and Li H. 1998. Post-collisional lithosphere delamination of the Dabie-Sulu orogen. Chinese Science Bulletin, 47 (3): 259 – 263

Li SR, Santosh M, Zhang HF, Shen JF, Dong GC, Wang JZ and Zhang JQ. 2013. Inhomogeneous lithospheric thinning in the central North China Craton: Zircon U-Pb and S-He-Ar isotopic record from magmatism and metallogeny in the Taihang Mountains. Gondwana Research, 23(1): 141 – 160

Li SZ, Zhao GC, Sun M, Han ZZ, Zhao GT and Hao DF. 2006. Are the South and North Liaohe groups of North China Craton different exotic terranes? Nd isotope constraints. Gondwana Research, 9(1 – 2): 198 – 208

Li SZ and Zhao GC. 2007. SHRIMP U-Pb zircon geochronology of the Liaoji granitoids: Constraints on the evolution of the Paleoproterozoic Jiao-Liao-Ji belt in the Eastern Block of the North China Craton. Precambrian Research, 158(1 – 2): 1 – 16

Li TS, Zhai MG, Peng P, Chen L and Guo JH. 2010. Ca. 2.5 billion year old coeval ultramafic-mafic and syenitic dykes in Eastern Hebei: Implications for cratonization of the North China Craton. Precambrian Research, 180(3 – 4): 143 – 155

Li XP, Yang ZY, Zhao GC, Grapes R and Guo JH. 2011. Geochronology of khondalite-series rocks of the Jining Complex: Confirmation of depositional age and tectonometamorphic evolution of the North China craton. International Geology Review, 53(10): 1194 – 1211

Lin W, Faure M, Monié P, Schärer U and Panis D. 2008. Mesozoic extensional tectonics in Eastern Asia: The south Liaodong peninsula metamorphic core complex (NE China). The Journal of Geology, 116(2): 134 – 154

Liu DY, Nutman AP, Compston W, Wu JS and Shen QH. 1992. Remnants of ≥3800Ma crust in the Chinese part of the Sino-Korean craton. Geology, 20(4): 339 – 342

Liu S. 2004. The Mesozoic magmatism and crustal extension in Shandong Province, China-additionally discussing the relationship between lamprophyres and gold mineralization. Ph. D. Dissertation. Guiyang: Institute of Geochemistry, Chinese Academy of Sciences (in Chinese with English abstract)

Liu S, Hu RZ, Zhao JH and Feng CX. 2004. K-Ar geochronology of Mesozoic mafic dikes in Shandong Province, eastern China: Implications for crustal extension. Acta Geologica Sinica, 78(6): 1207 – 1213

Liu S, Hu RZ, Zhao JH, Feng CX, Zhong H, Cao JJ and Shi DN. 2005. Geochemical characteristics and petrogenetic investigation of the Late Mesozoic lamprophyres of Jiaobei, Shandong Province. Acta Petrologica Sinica, 21(3): 947 – 958 (in Chinese with English abstract)

Liu S, Zou HB, Hu RZ, Zhao JH and Feng CX. 2006. Mesozoic mafic dikes from the Shandong Peninsula, North China Craton: Petrogenesis and tectonic implications. Geochemical Journal, 40 (2): 181 – 195

Liu S, Hu RZ, Gao S, Feng CX, Qi L, Zhong H, Xiao TF, Qi YQ, Wang T and Coulson IM. 2008a. Zircon U-Pb geochronology and major, trace elemental and Sr-Nd-Pb isotopic geochemistry of mafic dykes in western Shandong Province, East China: Constrains on their petrogenesis and geodynamic significance. Chemical Geology, 255(3 – 4): 329 – 345

Liu S, Hu RZ, Gao S, Feng CX, Qi YQ, Wang T, Feng GY and Coulson IM. 2008b. U-Pb zircon age, geochemical and Sr-Nd-Pb-Hf isotopic constraints on age and origin of alkaline intrusions and associated mafic dikes from Sulu orogenic belt, eastern China. Lithos, 106(3 – 4): 365 – 379

Liu S, Hu RZ, Gao S, Feng CX, Zhong H, Qi YQ, Wang T, Qi L and Feng GY. 2008c. K-Ar ages geochemical + Sr-Nd isotopic compositions of adakitic volcanic rocks, western Shandong Province, eastern China: Foundering of the lower continental crust. International Geology Review, 50(8): 763 – 779

Liu S, Hu RZ, Gao S, Feng CX, Yu BB, Feng GY, Qi YQ, Wang T and Coulson IM. 2009a. Petrogenesis of Late Mesozoic mafic dykes in the Jiaodong Peninsula, eastern North China Craton and implications for the foundering of lower crust. Lithos, 113(3 – 4): 621 – 639

Liu S, Hu RZ, Gao S, Feng CX, Yu BB, Qi YQ, Wang T, Feng GY and Coulson IM. 2009b. Zircon U-Pb age, geochemistry and Sr-Nd-Pb isotopic compositions of adakitic volcanic rocks from Jiaodong, Shandong Province, eastern China: Constraints on petrogenesis and implications. Journal of Asian Earth Sciences, 35(5): 445 – 458

Liu S, Hu RZ, Gao S, Feng CX, Feng GY, Qi YQ, Coulson IM, Yang YH, Yang CG and Tang L. 2012a. Geochemical and isotopic constraints on the age and origin of mafic dikes from eastern Shandong Province, eastern North China Craton. International Geology Review, 54(12): 1389 – 1400

Liu S, Hu RZ, Gao S, Feng CX, Coulson IM, Feng GY, Qi YQ, Yang YH, Yang CG and Tang L. 2012b. U-Pb zircon age, geochemical and Sr-Nd isotopic data as constraints on the petrogenesis and emplacement time of the Precambrian mafic dyke swarms in the North China Craton (NCC). Lithos, 140 – 141: 38 – 52

Liu S, Hu RZ, Gao S, Feng CX, Coulson IM, Feng GY, Qi YQ, Yang YH, Yang CG and Tang L. 2013a. Zircon U-Pb age and Sr-Nd-Hf isotopic constraints on the age and origin of Triassic mafic dikes, Dalian area, Northeast China. International Geology Review, 55 (2): 249 – 262

Liu S, Feng CX, Jahn BM, Hu RZ, Gao S, Coulson IM, Feng GY, Lai SC, Yang CG and Yang YH. 2013b. Zircon U-Pb age, geochemical, and Sr-Nd-Hf isotopic constraints on the origin of mafic dykes in the Shaanxi Province, North China Craton, China. Lithos, 175 – 176: 244 – 254

Liu S, Feng CX, Jahn BM, Hu RZ, Gao S, Feng GY, Lai SC, Yang YH, Qi YQ and Coulson IM. 2013c. Geochemical, Sr-Nd isotopic, and zircon U-Pb geochronological constraints on the petrogenesis of Late Paleoproterozoic mafic dykes within the northern North China Craton, Shanxi Province, China. Precambrian Research, 236: 182 – 192

Liu S, Feng CX, Jahn BM, Hu RZ, Gao S, Coulson IM, Feng GY, Lai SC, Yang YH and Tang L. 2013d. Geochemical, Sr-Nd-Pb isotope, and zircon U-Pb geochronological constraints on the origin of Early Permian mafic dikes, northern North China Craton. International Geology Review, 55(13): 1626 – 1640

Liu S, Hu RZ, Feng CX, Gao S, Feng GY, Lai SC, Qi YQ, Coulson IM, Yang YH, Yang CG and Tang L. 2013e. U-Pb zircon age, geochemical, and Sr-Nd-Pb isotopic constraints on the age and origin of mafic dykes from eastern Shandong Province, eastern China. Acta Geologica Sinica, 87(4): 1045 – 1057

Liu YS, Hu ZC, Zong KQ, Gao CG, Gao S, Xu J and Chen HH. 2010. Reappraisement and refinement of zircon U-Pb isotope and trace element analyses by LA-ICP-MS. Chinese Science Bulletin, 55 (15): 1535 – 1546

Ludwig KR. 2003. User's manual for Isoplot/Ex. Version 3.00: A Geochronological Toolkit for Microsoft Excel, 4. Berkeley: Berkeley Geochronology Center Special Publication, 1 – 70

Lugmair GW and Hairti K. 1972. Lunar initial $^{143}Nd/^{144}Nd$: Differential evolution of the lunar crust and mantle. Earth and Planetary Science Letters, 39(3): 349 – 457.

Luo Y, Sun M, Zhao GC, Li SZ, Ayers JC, Xia XP and Zhang JH. 2008. A comparison of U-Pb and Hf isotopic compositions of detrital zircons from the North and South Liaohe groups: Constraints on the evolution of the Jiao-Liao-Ji Belt, North China Craton. Precambrian Research, 163(3 – 4): 279 – 306

Ma F, Mu ZG and Li JH. 2000. Geochemistry and petrogenesis of Precambrian mafic dyke swarms. Geology-Geochemistry, 28(4): 58 – 64 (in Chinese with English abstract)

Meng QR and Zhang GW. 1999. Timing of collision of the North and South China blocks: Controversy and reconciliation. Geology, 27 (2): 123 – 126

Menzies MA and Kyle PR. 1972. Continental volcanism: A crust-mantle probe. In: Menzies MA (ed.). Continental Mantle. Oxford: Oxford University Press, 157 – 177

Menzies MA, Xu YG, Zhang HF and Fan WM. 2007. Integration of geology, geophysics and geochemistry: A key to understanding the North China Craton. Lithos, 96(1-2): 1-21

Middlemost EAK. 1994. Naming materials in the magma/igneous rock system. Earth-Science Reviews, 37(3-4): 215-224

Nisson MKM, Klausen MB, Söderlund U and Ernst RE. 2013. Precise U-Pb ages and geochemistry of Palaeoproterozoic mafic dykes from southern West Greenland: Linking the North Atlantic and the Dharwar cratons. Lithos, 174: 255-270

Oberthür T, Davis DW, Blenkinsop TG and Höhndorf A. 2002. Precise U-Pb mineral ages, Rb-Sr and Sm-Nd systematics for the Great Dyke, Zimbabwe-constraints on Late Archean events in the Zimbabwe craton and Limpopo belt. Precambrian Research, 113(3-4): 293-305

O'Brien PJ. 2001. Subduction followed by collision: Alpine and Himalayan examples. Physics of the Earth and Planetary Interiors, 127(1-4): 277-291

Peng P, Zhai MG, Zhang HF and Guo JH. 2005. Geochronological constraints on the Paleoproterozoic evolution of the North China Craton: SHRIMP zircon ages of different types of mafic dikes. International Geology Review, 47(5): 492-508

Peng P, Zhai MG, Guo JH, Kusky T and Zhao TP. 2007. Nature of mantle source contributions and crystal differentiation in the petrogenesis of the 1.78Ga mafic dykes in the central North China craton. Gondwana Research, 12(1-2): 29-46

Peng P, Zhai MG, Li Z, Wu FY and Hou QL. 2008. Neoproterozoic (~820Ma) mafic dyke swarms in the North China craton: Implication for a conjoint to the Rodinia supercontinent? In: Abstracts of 13th Gondwana Conference. Dali, China, 160-161

Peng P. 2010. Reconstruction and interpretation of giant mafic dyke swarms: A case study of 1.78Ga magmatism in the North China craton. Geological Society, London, Special Publication, 338: 163-178

Peng P, Guo JH, Zhai MG and Bleeker W. 2010. Paleoproterozoic gabbronoritic and granitic magmatism in the northern margin of the North China craton: Evidence of crust-mantle interaction. Precambrian Research, 183(3): 635-659

Peng P, Bleeker W, Ernst RE, Söderlund U and McNicoll V. 2011a. U-Pb baddeleyite ages, distribution and geochemistry of 925Ma mafic dykes and 900Ma sills in the North China craton: Evidence for a Neoproterozoic mantle plume. Lithos, 127(1-2): 210-221

Peng P, Zhai MG, Li QL, Wu FY, Hou QL, Li Z, Li TS and Zhang YB. 2011b. Neoproterozoic (~900Ma) Sariwon sills in North Korea: Geochronology, geochemistry and implications for the evolution of the south-eastern margin of the North China Craton. Gondwana Research, 20(1): 243-254

Piper JDA, Zhang JS, Huang BC and Roberts AP. 2011. Palaeomagnetism of Precambrian dyke swarms in the North China Shield: The ~1.8Ga LIP event and crustal consolidation in Late Palaeoproterozoic times. Journal of Asian Earth Sciences, 41(6): 504-524

Potts PJ and Kane JS. 2005. International association of geoanalysts certificate of analysis: Certified reference material OU-6 (Penrhyn slate). Geostandards and Geoanalytical Research, 29(2): 233-236

Qi L, Hu J and Grégoire DC. 2000. Determination of trace elements in granites by inductively coupled plasma mass spectrometry. Talanta, 51(3): 507-513

Rapp RP, Shimizu N and Norman MD. 2003. Growth of early continental crust by partial melting of eclogite. Nature, 425(6958): 605-609

Shao JA and Zhang LQ. 2002. Mesozoic dyke swarms in the north of North China. Acta Petrologica Sinica, 18(3): 312-318 (in Chinese with English abstract)

Shao JA, Zhang YB, Zhang LQ, Mu BL, Wang PY and Guo F. 2003. Early Mesozoic dike swarms of carbonatites and lamprophyres in Datong area. Acta Petrologica Sinica, 19(1): 93-104 (in Chinese with English abstract)

Skjerlie KP and Douce AEP. 2002. The fluid-absent partial melting of a zoisite-bearing quartz eclogite from 1.0 to 3.2GPa: Implications for melting in thickened continental crust and for subduction-zone processes. Journal of Petrology, 43(2): 291-314

Steiger RH and Jager E. 1977. Subcommission on geochronology: Convention on the use of decay constraints in geochronology and cosmochronology. Earth and Planetary Science Letters, 36: 359-362

Sun SS and McDonough WF. 1989. Chemical and isotopic systematics of oceanic basalts: Implications for mantle composition and processes. In: Saunders AD and Norry MJ (eds.). Magmatism in the Ocean Basins. Geological Society, London, Special Publications, 42(1): 313-345

Tam PY, Zhao GC, Liu FL, Zhou XW, Sun M and Li SZ. 2011. Timing of metamorphism in the Paleoproterozoic Jiao-Liao-Ji Belt: New SHRIMP U-Pb zircon dating of granulites, gneisses and marbles of the Jiaobei massif in the North China Craton. Gondwana Research, 19(1): 150-162

Tam PY, Zhao GC, Zhou XW, Sun M, Guo JH, Li SZ, Yin CQ, Wu ML and He YH. 2012a. Metamorphic P-T path and implications of high-pressure pelitic granulites from the Jiaobei massif in the Jiao-Liao-Ji Belt, North China Craton. Gondwana Research, 22(1): 104-117

Tam PY, Zhao GC, Sun M, Li SZ, Wu ML and Yin CQ. 2012b. Petrology and metamorphic P-T path of high-pressure mafic granulites from the Jiaobei massif in the Jiao-Liao-Ji Belt, North China Craton. Lithos, 155: 94-109

Tang YJ, Zhang HF, Santosh M and Ying JF. 2013. Differential destruction of the North China Craton: A tectonic perspective. Journal of Asian Earth Sciences, 78: 71-82

Tarney J and Weaver BL. 1987. Geochemistry and petrogenesis of Early Proterozoic dyke swarms. In: Halls HC and Fahrig WF (eds.). Mafic Dyke Swarms. Special Publication-Geological Association of Canada, 34: 81-93

Thompson M, Potts PJ, Kane JS and Wilson S. 2000. GeoPT5: An international proficiency test for analytical geochemistry laboratories-report on round 5. Geostandards Newsletter, 24(1): E1-E28

Wang F, Li XP, Chu H and Zhao GC. 2011. Petrology and metamorphism of khondalites from the Jining Complex, North China Craton. International Geology Review, 53(2): 212-229

Wang LG, Qiu YM, McNaughton NJ, Groves DI, Luo ZK, Huang JZ, Miao LC and Liu YK. 1998. Constraints on crustal evolution and gold metallogeny in the Northwestern Jiaodong Peninsula, China, from SHRIMP U-Pb zircon studies of granitoids. Ore Geology Reviews, 13(1-5): 275-291

Wang T, Zheng YD, Zhang JJ, Wang XS, Zeng LS and Tong Y. 2007. Some problems in the study of Mesozoic extensional structure in the North China Craton and its significance for the study of lithospheric thinning. Geological Bulletin of China, 26(9): 1154-1166 (in Chinese with English abstract)

Wang YJ, Fan WM, Peng TP, Zhang HF and Guo F. 2005. Nature of the Mesozoic lithospheric mantle and tectonic decoupling beneath the Dabie Orogen, Central China: Evidence from $^{40}Ar/^{39}Ar$ geochronology: Elemental and Sr-Nd-Pb isotopic compositions of Early Cretaceous mafic igneous rocks. Chemical Geology, 220(3-4): 165-189

Wang YJ, Zhang YZ, Zhao GC, Fan WM, Xia XP, Zhang FF and Zhang AM. 2009. Zircon U-Pb geochronological and geochemical constraints on the petrogenesis of the Taishan sanukitoids (Shandong): Implications for Neoarchean subduction in the eastern block, North China Craton. Precambrian Research, 174(3-4): 273-286

Wilde SA, Zhao GC and Sun M. 2002. Development of the North China craton during the Late Archaean and its final amalgamation at 1.8Ga: Some speculations on its position within a global Palaeoproterozoic Supercontinent. Gondwana Research, 5(1): 85-94

Wu FY, Lin JQ, Wilde SA, Zhang XQ and Yang JH. 2005. Nature and significance of the Early Cretaceous giant igneous event in eastern

China. Earth and Planetary Science Letters, 233(1-2): 103-119

Wu FY, Yang YH, Xie LW, Yang JH and Xu P. 2006. Hf isotopic compositions of the standard zircons and baddeleyites used in U-Pb geochronology. Chemical Geology, 234(1-2): 105-126

Wu FY, Xu YG, Gao S and Zheng JP. 2008. Lithospheric thinning and destruction of the North China Craton. Acta Petrologica Sinica, 24(6): 1145-1174 (in Chinese with English abstract)

Wu KK, Zhao GC, Sun M, Yin CQ, He YH and Tam PY. 2013a. Metamorphism of the northern Liaoning Complex: Implications for the tectonic evolution of Neoarchean basement of the eastern block, North China Craton. Geoscience Frontiers, 4(3): 305-320

Wu ML, Zhao GC, Sun M, Li SZ, He YH and Bao Z. 2013b. Zircon U-Pb geochronology and Hf isotopes of major lithologies from the Yishui Terrane: Implications for the crustal evolution of the eastern block, North China Craton. Lithos, 170-171: 164-178

Xia XP, Sun M, Zhao GC, Wu FY, Xu P, Zhang J and He YH. 2008. Paleoproterozoic crustal growth in the Western Block of the North China Craton: Evidence from detrital zircon Hf and whole rock Sr-Nd isotopic compositions of the khondalites from the Jining Complex. American Journal of Science, 308(3): 304-327

Xie GQ. 2003. Geological and geochemical feature of the mafic dykes since Late Mesozoic and its geodynamic significance, Jiangxi Province, southeastern China. Ph. D. Dissertation. Guiyang: Institute of Geochemistry, Chinese Academy of Sciences (in Chinese)

Xu JW, Ma GF, Tong WX, Zhu G and Lin SF. 1993. Displacement of the Tancheng-Lujiang wrench fault system and its geodynamic setting in the northwestern Circum-Pacific. In: Xu J (ed.). The Tancheng-Lujiang Wrench System. New York: John Wiley & Sons, 51-74

Xu YG. 2004. Lithospheric thinning beneath North China: A temporal and spatial perspective. Geological Journal of China Universities, 10(3): 324-331 (in Chinese with English abstract)

Yang JH, Wu FY and Wilde SA. 2003. A review of the geodynamic setting of large-scale Late Mesozoic gold mineralization in the North China Craton: An association with lithospheric thinning. Ore Geology Reviews, 23(3-4): 125-152

Yang JH, Chung SL, Zhai MG and Zhou XH. 2004. Geochemical and Sr-Nd-Pb isotopic compositions of mafic dikes from the Jiaodong Peninsula, China: Evidence for vein-plus-peridotite melting in the lithospheric mantle. Lithos, 73(3-4): 145-160

Yaxley GM. 2000. Experimental study of the phase and melting relations of homogeneous basalt + peridotite mixtures and implications for the petrogenesis of flood basalts. Contributions to Mineralogy and Petrology, 139(3): 326-338

Ye K, Cong BL and Ye DN. 2000. The possible subduction of continental material to depths greater than 200km. Nature, 407(6805): 734-736

Yin CQ, Zhao GC, Sun M, Xia XP, Wei CJ, Zhou XW and Leung WH. 2009. LA-ICP-MS U-Pb zircon ages of the Qianlishan Complex: Constrains on the evolution of the Khondalite Belt in the Western Block of the North China Craton. Precambrian Research, 174(1-2): 78-94

Yin CQ, Zhao GC, Guo JH, Sun M, Xia XP, Zhou XW and Liu CH. 2011. U-Pb and Hf isotopic study of zircons of the Helanshan Complex: Constrains on the evolution of the Khondalite Belt in the Western Block of the North China Craton. Lithos, 122(1-2): 25-38

Yuan HL, Gao S, Liu XM, Li HM, Günther D and Wu FY. 2004. Accurate U-Pb age and trace element determinations of zircon by laser ablation-inductively coupled plasma-mass spectrometry. Geostandards and Geoanalytical Research, 28(3): 353-370

Zhai MG, Fang HR, Yang JH and Miao LC. 2004. Large-scale cluster of gold deposits in East Shandong: Anorogenic metallogenesis. Earth Science Frontiers, 11(1): 85-98 (in Chinese with English abstract)

Zhai MG and Santosh M. 2011. The Early Precambrian odyssey of the North China Craton: A synoptic overview. Gondwana Research, 20(1): 6-25

Zhai MG and Santosh M. 2013. Metallogeny of the North China Craton: Link with secular changes in the evolving Earth. Gondwana Research, 24(1): 275-297

Zhang CH. 2009. Selected tectonic topics in the investigation of geodynamic process of destruction of North China Craton. Earth Science Frontiers, 16(4): 203-214 (in Chinese with English abstract)

Zhang GS. 2006. Chronology, geochemistry and geodynamic significance of the mafic-ultramafic rocks in Fujian Province since Late Mesozoic. Ph. D. Dissertation. Guiyang: Institute of Geochemistry, Chinese Academy of Sciences (in Chinese)

Zhang HF and Sun M. 2002. Geochemistry of Mesozoic basalts and mafic dikes, southeastern north China Craton, and tectonic implications. International Geology Review, 44(4): 370-382

Zhang HF, Sun M, Zhou MF, Fan WM, Zhou XH and Zhai MG. 2004. Highly heterogeneous Late Mesozoic lithospheric mantle beneath the North China Craton: Evidence from Sr-Nd-Pb isotopic systematics of mafic igneous rocks. Geological Magazine, 141(1): 55-62

Zhang HF, Sun M, Zhou XH and Ying JF. 2005. Geochemical constraints on the origin of Mesozoic alkaline intrusive complexes from the North China Craton and tectonic implications. Lithos, 81(1-4): 297-317

Zhao GC, Wilde SA, Cawood PA and Sun M. 2001. Archean blocks and their boundaries in the North China Craton: Lithological, geochemical, structural and *P-T* path constraints and tectonic evolution. Precambrian Research, 107(1-2): 45-73

Zhao GC, Sun M, Wilde SA and Li SZ. 2005. Late Archean to Paleoproterozoic evolution of the North China craton: Key issues revisited. Precambrian Research, 136(2): 177-202

Zhao GC. 2009. Metamorphic evolution of major tectonic units in the basement of the North China Craton: Key issues and discussion. Acta Petrologica Sinica, 25(8): 1772-1792 (in Chinese with English abstract)

Zhao GC, Wilde SA, Guo JH, Gawood PA, Sun M and Li XP. 2010. Single zircon grains record two Paleoproterozoic collisional events in the North China Craton. Precambrian Research, 177(3-4): 266-276

Zhao GC, Gawood PA, Li SZ, Wilde SA, Sun M, Zhang J, He YH and Yin CQ. 2012. Amalgamation of the North China Craton: Key issues and discussion. Precambrian Research, 222-223: 55-76

Zhao GC and Zhai MG. 2013. Lithotectonic elements of Precambrian basement in the North China Craton: Review and tectonic implications. Gondwana Research, 23(4): 1207-1240

Zhao JH. 2004. The discussion on the Mesozoic mafic dykes from Fujian province, China. Ph. D. Dissertation. Guiyang: Institute of Geochemistry, Chinese Academy of Sciences (in Chinese)

Zhao JX and McCulloch MT. 1993. Melting of a subduction-modified continental lithospheric, mantle: Evidence from late Proterozoic mafic dike swarms, in central Australia. Geology, 21(5): 463-466

Zheng JP, Griffin WL, O'Reilly SY, Lu FX, Wang CY, Zhang M, Wang FZ and Li HM. 2004. 3.6Ga lower crust in central China: New evidence on the assembly of the North China Craton. Geology, 32(3): 229-232

Zheng YF, Xiao WJ and Zhao GC. 2013. Introduction to tectonics of China. Gondwana Research, 23(4): 1189-1206

Zhou XW, Zhao GC, Wei CJ, Geng YS and Sun M. 2008. EPMA U-Th-Pb monazite and SHRIMP U-Pb zircon geochronology of high-pressure pelitic granulites in the Jiaobei massif of the North China Craton. American Journal of Science, 308(3): 328-350

附中文参考文献

曹建劲. 2007. 广东和海南省新生代基性岩墙地球化学和岩石圈演化. 博士学位论文. 贵阳: 中国科学院地球化学研究所

陈孝德, 史兰斌, 贾三发. 1992. 华北元古代基性岩墙群研究. 地震地质, 14(4): 351-357

李超文，郭锋，李晓勇．2004．溧水盆地晚中生代基性火山岩成因与深部动力学过程探讨．地球化学，33(4)：361－371

刘燊．2004．山东地区中生代岩浆作用与地壳拉张：兼论煌斑岩与金成矿的关系．博士学位论文．贵阳：中国科学院地球化学研究所

刘燊，胡瑞忠，赵军红，冯彩霞，钟宏，曹建劲，史丹妮．2005．胶北晚中生代煌斑岩的岩石地球化学特征及其成因研究．岩石学报，21(3)：947－958

马芳，穆治国，李江海．2000．前寒武纪基性岩墙群的地球化学特征与岩石成因讨论．地质地球化学，28(4)：58－64

邵济安，张履桥．2002．华北北部中生代岩墙群．岩石学报，18(3)：312－318

邵济安，张永北．2003．大同地区早中生代煌斑岩-碳酸岩岩墙群．岩石学报，19(1)：93－104

王涛，郑亚东，张进江，王新摄，曾令森，童英．2007．华北克拉通中生代伸展构造研究的几个问题及其在岩石圈减薄研究中的意义．地质通报，26(9)：1154－1166

吴福元，徐义刚，高山，郑建平．2008．华北岩石圈减薄与克拉通破坏研究的主要学术争论．岩石学报，24(6)：1145－1174

谢桂青．2003．江西省中生代基性岩墙地质地球化学特征及其地球动力学意义．博士学位论文．贵阳：中国科学院地球化学研究所

徐义刚．2004．华北岩石圈减薄的时空不均一特征．中国地质大学学报，10(3)：324－331

翟明国，范宏瑞，杨进辉，苗来成．2004．非造山带型金矿——胶东型金矿的陆内成矿作用．地学前缘，11(1)：85－98

张长厚．2009．华北克拉通破坏动力学过程研究中的几个构造问题．地学前缘，16(4)：203－214

张贵山．2006．福建晚中生代以来基性-超基性岩的年代学、地球化学及其地球动力学意义．博士学位论文．贵阳：中国科学院地球化学研究所

赵国春．2009．华北克拉通基底主要构造单元变质作用演化及其若干问题讨论．岩石学报，25(8)：1772－1792

赵军红．2004．福建省中生代基性岩墙探讨．博士学位论文．贵阳：中国科学院地球化学研究所